

U.S. DEPARTMENT OF COMMERCE
National Technical Information Service

AD-A032 963

THE PERFORMANCE OF TWO BOEING-GM WHEELS
(GM VII AND GM VIII) FOR THE MANNED
LUNAR ROVER VEHICLE

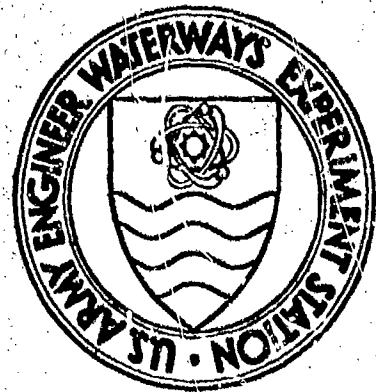
ARMY ENGINEER WATERWAYS EXPERIMENT
STATION, VICKSBURG, MISSISSIPPI

FEBRUARY 1971

TA7

1434m

1-71-3



0

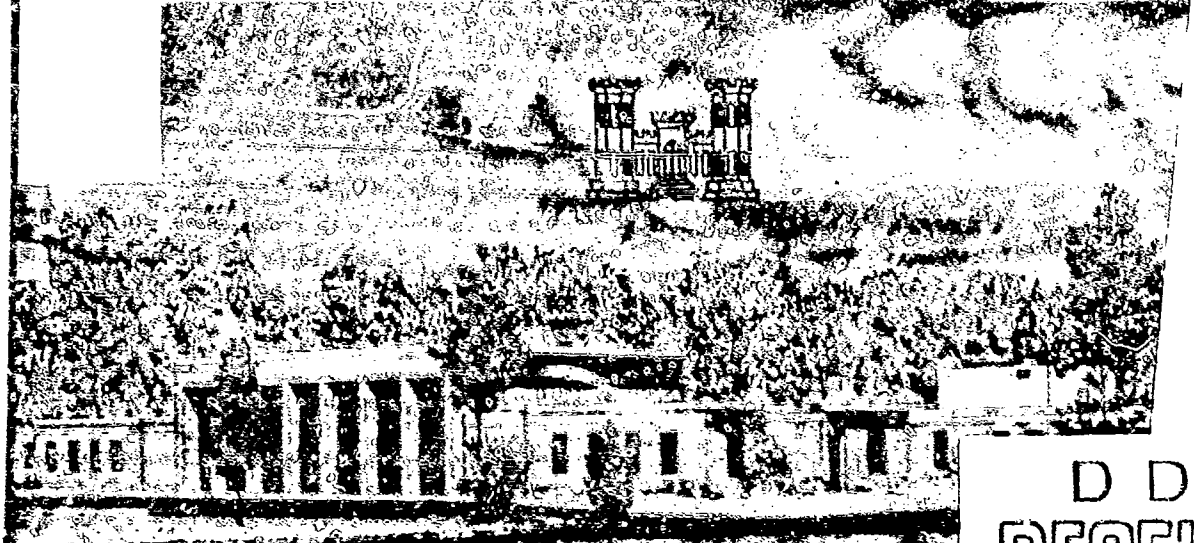
ADA 032963

MISCELLANEOUS PAPER M-71-3

**THE PERFORMANCE OF TWO BOEING-GM
WHEELS (GM VII AND GM VII!) FOR THE
MANNED LUNAR ROVER VEHICLE**

by

A. J. Green, K. J. Malzer



REPRODUCED BY
NATIONAL TECHNICAL
INFORMATION SERVICE
U. S. DEPARTMENT OF COMMERCE
SPRINGFIELD, VA. 22161

DDC
RECEIVED
DEC 9 1976
D

February 1971

Approved by George C. Marshall Space Flight Center
National Aeronautics and Space Administration, Huntsville, Alabama

Conducted by U. S. Army Engineer Waterways Experiment Station, Vicksburg, Mississippi

This document has been approved for public release and sale; its distribution is unlimited

54

Destroy this report when no longer needed. Do not return
it to the originator.

The findings in this report are not to be construed as an official
Department of the Army position unless so designated
by other authorized documents.

TAN
W34m
No. M-71-3

THE CONTENTS OF THIS REPORT ARE NOT TO BE
USED FOR ADVERTISING, PUBLICATION, OR
PROMOTIONAL PURPOSES. CITATION OF TRADE
NAMES DOES NOT CONSTITUTE AN OFFICIAL EN-
DORSEMENT OR APPROVAL OF THE USE OF SUCH
COMMERCIAL PRODUCTS.

Preceding page blank

FOREWORD

The study reported herein was conducted by personnel of the Mobility Research Branch (MRB), Mobility and Environmental (M&E) Division, U. S. Army Engineer Waterways Experiment Station (WES). The study was sponsored by the Lunar Exploration Office, National Aeronautics and Space Administration, Washington, D. C., and it was under the technical cognizance of Dr. N. C. Costes of the Space Sciences Laboratory, George C. Marshall Space Flight Center (MSFC), Huntsville, Ala. The work was performed under NASA - Defense Purchase Request No. H-65056A, dated 16 December 1969.

The tests were conducted under the general supervision of Messrs. W. C. Shockley and S. J. Knight, Chief and Assistant Chief, respectively, of the M&E Division; and under the direct supervision of Mr. A. J. Green and Dr. K.-J. Melzer of the Research Projects Group, MRB. This report was prepared by Mr. Green and Dr. Melzer.

The wheels used in this study were furnished by the A. C. Electronics Division of General Motors Corporation in cooperation with the Boeing Company (Huntsville, Ala.) and MSFC.

Acknowledgment is made to Dr. D. R. Freitag, Assistant Technical Director, WES, for his advice and assistance during this study.

COL Levi A. Brown, CE, and COL Ernest D. Peixotto, CE, were Directors of WES during the conduct of this study and preparation of this report. Mr. F. R. Brown was Technical Director.

Preceding page blank

CONTENTS

| | <u>Page</u> |
|--|-------------|
| FOREWORD | v |
| NOTATION | ix |
| SUMMARY | xiii |
| PART I: INTRODUCTION | 1 |
| Background | 1 |
| Purpose and Scope | 2 |
| PART II: TEST PROGRAM | 3 |
| Soil | 3 |
| Test Equipment | 4 |
| Test Procedures and Interpretation of Data | 4 |
| PART III: PRESENTATION AND ANALYSIS OF RESULTS | 6 |
| Soil Tests | 6 |
| Performance of the Fabric-Covered Wheel (GM VII) | 6 |
| Performance of the Open-Wire-Mesh Wheel (GM VIII) | 8 |
| Comparative Performance of Covered and Open Wheels | 10 |
| PART IV: CONCLUSIONS | 12 |
| TABLES 1-4 | |
| FIGURES 1-28 | |

Preceding page blank

NOTATION

(Reproduced from WES Technical Report M-70-2, "Performance of Wheels for Lunar Vehicles." Many symbols shown are not used in this report.)

- A Shear area, cm^2 (in.²)
- A_c Hard-surface contact area, cm^2 (in.²)
- A_g Active grouser area, cm^2 (in.²)
- b Width of wheel; width of grouser, cm (in.)
- c Cohesion of the soil, kN/m^2 (psi)
- c_a Apparent cohesion of the soil, kN/m^2 (psi)
- c_b Cohesion determined from bevameter tests, kN/m^2 (psi)
- c_c Cohesion determined from sheargraph tests, kN/m^2 (psi)
- c_{pl} Cohesion determined from plate in situ shear tests, kN/m^2 (psi)
- c_t Cohesion corresponding to tangent friction angle, kN/m^2 (psi)
- c_{tr} Cohesion determined from trenching tests, kN/m^2 (psi)
- C_a Force due to apparent cohesion of the soil, N (lb)
- C_u Coefficient of uniformity of the soil = d_{60}/d_{10}
- d Wheel diameter, cm (in.)
- d_m Mean diameter of soil grains, mm (in.)
- d_{60} Grain-size diameter at 60 percent finer by weight, mm (in.)
- D Depth, cm (in.)
- D' Compactibility, % = $100 \left(\frac{e_{\max} - e_{\min}}{e_{\min}} \right)$
- D_r Relative density, % = $100 \left(\frac{e_{\max} - e}{e_{\max} - e_{\min}} \right)$
- e Initial void ratio
- e_{\max} Maximum void ratio
- e_{\min} Minimum void ratio
- F Friction force, N (lb)
- G Penetration resistance gradient, KN/m^3 (pci*)
- k_c, k_ϕ, n Bekker soil values
- k_d Count ratio (wet density)
- k_m Count ratio (moisture content)
- M Torque, m-N (ft-lb)
- N_g Number of grousers embedded in soil
- P Pull, N (lb)

*pci = lb/in.^3

| | |
|----------------------|---|
| PN | Power number, $M/Wr_e(1 - s)$ |
| q_c | Cone penetration resistance, kN/m^2 (psi) |
| r | Radius of shear head, cm (in.) |
| r_e | Effective wheel radius, cm (in.) |
| R | Length of torque arm, cm (in.) |
| R_p | Ratio of performance P_{20}/W (modified wheel/original wheel) |
| R_{pl}, R'_{pl} | Soil potential ratios (modified wheel/original wheel) for plate in situ shear tests |
| R_t, R'_t | Soil potential ratios (modified wheel/original wheel) for vacuum triaxial tests |
| s | Slip, % |
| s_A | Average settlement of the plate in the in situ shear tests |
| s_b | Shear stress determined from bevameter tests, kN/m^2 (psi) |
| s_c | Shear stress determined from sheargraph tests, kN/m^2 (psi) |
| s_v | Shear stress determined from vane shear tests, kN/m^2 (psi) |
| S | Soil potential |
| S_{pl}, S'_{pl} | Soil potential (plate in situ shear tests) |
| S_t, S'_t | Soil potential (vacuum triaxial tests) |
| v | Translational speed of a wheel, m/sec (fps) |
| V | Volume |
| w | Moisture content, % (percent of dry density) |
| w' | Moisture content, g/cm^3 (pcf) (mass per volume) |
| W | Load; weight, N (lb) |
| z | Grouser height, cm (in.) |
| α | Slope angle, deg |
| γ | Wet density, g/cm^3 (pci) |
| γ_d | Dry density, g/cm^3 (pci) |
| γ_s | Specific gravity |
| Δl | Horizontal displacement of the plate in the in situ shear tests |
| $\Delta V/V$ | Volume change, % |
| e | Axial strain, % |
| η' | Efficiency = ratio of recoverable energy to total energy input |
| λ_p | Passive earth pressure factor for Rankine case |
| σ | Stress, kN/m^2 (psi) |
| σ_1 | Major principal stress, kN/m^2 (psi) |
| σ_2, σ_3 | Minor principal stresses, kN/m^2 (psi) |
| σ_n | Normal stress, kN/m^2 (psi) |

Preceding page blank

τ Shear stress, kN/m^2 (psi)
 τ_v Energy component of total shear stress
 ϕ Friction angle, deg
 ϕ_b Friction angle determined from beyameter tests, deg
 ϕ_c Friction angle determined from sheargraph tests, deg
 ϕ_{ds} Friction angle determined from direct shear tests, deg
 ϕ_p Peak friction angle determined from plane strain tests, deg
 ϕ_{pl} Friction angle determined from plate in situ shear tests, deg
 ϕ_r True friction angle, deg
 ϕ_s Secant friction angle determined from triaxial tests, deg
 ϕ_t Tangent friction angle determined from triaxial tests, deg
 ω Rotational velocity of the wheel, rpm

SUMMARY

Two candidate wheels for the Boeing-GM Manned Lunar Rover Vehicle, one fabric-covered and one constructed of open-wire mesh, were tested for mobility performance in a fine sand. Four levels of sand strength, representing cohesion values ranging from zero to 0.16 psi, were used in the tests. The cohesive and frictional properties of the sand spanned a range that is believed to include the probable range of lunar soil properties.

A dynamometer system was used to conduct programmed-slip tests with the wheels. The slip was varied from a negative slip of 15% to a positive slip of 100%. The wheels were tested at the average design load (59 lb) and at 75 and 125% of that load, so the influence of load imbalance and dynamic load transfer could be assessed. The average speed at 0 percent slip was 3 ft/sec.

The test results show that the covered wheel was able to achieve the desired tractive performance (pull/weight ratio = 0.47, equivalent to climbing a 25-deg slope) in the two strongest soil conditions, but not in the two weakest ones. The open wheel was not able to achieve this tractive performance in any of the soil conditions tested. In the same soil condition, the maximum pull/weight ratio for the open wheel was consistently less than that for the covered wheel.

The power required to attain a given level of tractive performance (below the maximum for a given wheel) was about the same for both wheels in all soil conditions. The power requirement was greater on the weaker soils than on the stronger, and it increased almost linearly with increasing pull/weight ratio. On level soil, each wheel required about 7 whr/km at the nominal rated load of 59 lb.

There was no consistent difference in the dimensionless performance ratios (pull/weight, power number, efficiency) as a direct result of any of the three loads used. Thus, the effects of moderate load imbalances do not appear critical.

The soil condition designated C_0 was easily compacted by passage of the wheel. The results of one test with each wheel in this soil condition showed that the covered wheel compacted the soil to a denser state than the open wheel did.

THE PERFORMANCE OF TWO BOEING-GM WHEELS (GM VII AND GM VIII)
FOR THE MANNED LUNAR ROVER VEHICLE

PART I: INTRODUCTION

Background

1. Tests conducted in the summer of 1969 by the U. S. Army Engineer Waterways Experiment Station (WES) to quantify the performance of the 40-in. diam Bendix, Boeing-GM, and Grumman wheels indicated that the latter two wheels (as delivered to WES) did not meet the requirements for slope-climbing ability, i.e. 25 deg on sandy soil. Accordingly, during the course of that test program, simple modifications of these two wheels were made in an attempt to improve their performance. In the case of the Boeing-GM wheel, it was demonstrated that both reducing the stiffness of the wheel and adding a fabric cover to it improved its performance. These tests are fully reported in WES Technical Report No. M-70-2.*

2. After the contract for the Manned Lunar Rover Vehicle (MLRV) system was awarded to The Boeing Company, its subcontractor, General Motors Corporation, fabricated two new 40-in.-diam wheels, one with inner and outer wire-mesh surfaces separated by a layer of fabric and with traction spikes attached to the outer surface, and the other of open wire mesh and with chevron metal treads (see fig. 1). At the

*Freitag, D. R., Green, A. J., and Felzer, K.-J., "Performance Evaluation of Wheels for Lunar Vehicles," Technical Report No. M-70-2, March 1970, U. S. Army Engineer Waterways Experiment Station, CE, Vicksburg, Mississippi.

request of the George C. Marshall Space Flight Center (MSFC), WES conducted tests to evaluate the performance of these two wheels. The results are reported herein.

Purpose and Scope

3. The purpose of this test program was to determine the quantitative performance of the fabric-covered wheel (GM VII) and the open-wire-mesh wheel (GM VIII). The test program consisted of a series of single-wheel programmed-slip tests in the same sand used in the earlier tests*. As had been done in these earlier tests, the consistency of the sand was varied to cover a range of cohesive and frictional properties to simulate soil conditions assumed to exist on the moon. Four soil conditions, S_1 , C_0 , C'_1 , and C_2 (see table 1), were used in the test program. Initially, tests were to be conducted on each soil condition at 50, 75, 100, 125, and 150% of the design load of 55-60 lb. However, by mutual agreement, testing at 50 and 150% of the design loads was deferred. The same soil, wheel, and wheel-performance parameters measured in earlier tests were measured in this test program.

*Ibid., p 1.

PART II: TEST PROGRAM

Soil

Description

4. The soil used in this study was a fine dune sand from the desert near Yuma, Arizona. It was classified SP-SM according to the Unified Soil Classification System. Gradation and classification data, together with density and void ratio values, are given in fig. 2. This soil is primarily cohesionless, but it exhibits a small amount of cohesion, particularly when damp.

Preparation

5. Level surfaces. The desired soil condition in dry sand was obtained in the following manner: The test bins were filled and the soil was plowed with a seed fork to a depth of 12 in. For loose conditions, no compaction effort was necessary, so the surface of the plowed section was screeded level; for the denser conditions, compaction was applied at the surface with a vibrator before screeding. The relation between dry density and relative density for the material is shown in fig. 3.

6. To prepare the wet sand, a batch of dry sand was spread on the floor, water was added, and the material was thoroughly mixed until the desired moisture content was reached. The material was then dumped into the bins for further processing (i.e. compacting and levelling), which was the same as for the dry sand. The moisture level in these sections was held constant by covering them when not in use and occasionally

spraying the surface very lightly with water to compensate for evaporation. The wet soil was reprocessed in place, being removed from the soil bins only when a different level of moisture was required. During the testing cycles in this test program, the uniformity of soil conditions was ensured by frequent determination of moisture content and density and by measurements with the cone penetrometer.

Test Equipment

7. The dynamometer system used in these tests can accommodate loads from approximately 15 to slightly more than 200 lb., and wheels ranging from 18 in. to 45 in. in diameter. Vertical load, horizontal force (drawbar pull), torque, sinkage, carriage speed, and wheel speed were continuously measured during each test by instrumentation on the dynamometer carriage. The average translational wheel speed at 0 percent slip was approximately 3 ft/sec; the rotational speed was constant.

Test Procedures and Interpretation of Data

8. A programmed-slip technique was used in all the single-wheel tests. The test was started when the wheel was in the negative slip range, i.e. the translational speed of the carriage was greater than that of the wheel. The carriage was slowed at a programmed, uniform rate (wheel speed was approximately constant) to cause the wheel to pass through the zero-torque point, the 0% slip point, the self-propelled point, etc., as slip progressively increased to 100%.

9. The relation of pull and torque to slip can be shown by two curves, such as those in fig. 4 that represent data obtained with the open-mesh wheel (GM VIII). Pull and torque increased at a decreasing rate and often reached a plateau after a slip of about 20% had been achieved. Although all tests were not identical, pull and torque in nearly all of them had reached a plateau, or significantly lower rate of increase, at a slip of 20%, so data for comparing performance of the two wheels were read at 20% slip.

10. The general shape of the efficiency versus slip curve for the GM VIII wheel is shown in fig. 5. This relation was generally similar to that for the GM VII wheel. However, in some instances, a peak efficiency point was difficult to determine. For consistency and ease of comparison, efficiency at 20% slip was recorded for all the tests.

11. The plot of the power number $PN \left[\frac{H}{Wr_e (1-s)} \right]$ versus the pull coefficient P/W (see fig. 6) is especially important, since it expresses the energy consumed per unit of distance per unit of wheel or vehicle weight in relation to drawbar pull/slope-climbing ability. PN at 0 pull, PN on a 15-deg slope (PN_{15}), PN on a 25-deg slope (PN_{25}), and PN at the point on the curve where PN ascends almost vertically (PN_{max}) were recorded. To obtain whr/km conforming to a slope of 15 deg, read the value of PN_{15} or $P/W = 0.27$ ($\tan 15^\circ = 0.27$), and multiply this value by the desired wheel load or vehicle weight in Newtons and the fraction 1000/3600.

PART III: PRESENTATION AND ANALYSIS OF RESULTS

Soil Tests

12. The soil tests conducted in this program included cone and plate penetration resistance, moisture content, density, plate in-situ shear with a rough-surfaced rectangular plate, and plate in-situ shear data collected previously.*

13. Values of the following parameters pertinent to the tests reported herein are contained in table 1: penetration resistance gradient, G ; bevameter values, k_c , k_ϕ , n , ϕ_b , and c_b ; cohesion from trenching tests, c_{tr} ; tangent friction angle from triaxial tests, ϕ_t ; friction angle from plate in-situ shear test, ϕ_{pl} ; density, γ , relative density, D_r ; and moisture content, w .

Performance of the Fabric-Covered Wheel (GH VII)

Pull and torque

14. The relations of the pull and torque coefficients to slip on soil prepared to four different consistencies are shown in figs. 7-10. The following observations can be made:

- a. The rate of increase in pull and torque coefficients with slip in the 0-20% slip range generally increased with soil strength, and the point at which the slope of the torque-slip and pull-slip relations changed rapidly was reached at a lower slip in the stronger materials.

*Ibid., p 1.

For example, this point was reached at about 15% slip on the C_2 soil condition ($G = 12.0$ psi/in.), and at slightly greater than 20% slip on the S_1 soil condition ($G = 2.0$ psi/in.).

- b. There was no clear-cut tendency for the wheel to perform better at the design load than at the other loads (75 and 125% of design load).
- c. The pull-slip curves did not display the well-defined plateaus that were noted for the 40-in.-diam wheels tested in the earlier program.* Instead, they showed a gradual increase in pull coefficient with slip in the 20-80% range.

Power number versus pull coefficient/slope-climbing ability

15. Plots of power number versus pull coefficient/slope angle for the test loads on each of the four soil conditions are shown in figs. 11-14.

The following observations can be made:

- a. Power number increased directly with pull coefficient (or slope angle) to a maximum, or near maximum, value of the latter dual parameter and then rose almost vertically.
- b. No significant or consistent effect of load per se was evident.
- c. The power number between zero and the maximum pull coefficient (or slope angle) generally was higher for the two lower soil strengths (C_0, S_1) than for the two higher strengths (C_1, C_2).

16. The curves in figs. 11-14 can be used to compute the power

* Ibid., p 1.

consumption rate on level and sloping surfaces by the formula

$$\text{Power consumption rate} = PN \times \frac{1000}{3600} = \text{load (N)}$$

in units of whr/km/wheel

For example, from fig. 11, the power number for a 59-lb (260-N) load on a 15-deg slope is read to be 0.46. Thus the power consumption rate (per wheel) is

$$0.46 \times \frac{1000}{3600} \times 260 = 33.3 \text{ whr/km/wheel}$$

Efficiency

17. The relative efficiency of the wheel is shown in table 2. In terms of the ratio of output work to input work at the 20% slip point, efficiency is expressed:

$$n'_{20} = \frac{P/W}{M/Wr_e} (1-s) = \frac{Pr_e}{M} (1-s) = \frac{Pr_e}{M} \cdot 0.8$$

It is noted that n' does not vary noticeably with load, but does show an increase as soil strength increases. This trend supports the reasoning that more work is dissipated in deforming the weaker soils.

Sinkage

18. In general, sinkages were small. The greatest sinkage occurred during tests in the C_0 soil condition. The relation of sinkage to slip for a 59-lb load in the C_0 soil condition is shown in fig. 15.

Performance of the Open-Wire-Mesh Wheel (GM VIII)

Pull and torque

19. The relations of the pull and torque coefficients to slip for the GM VIII wheel tested on soil prepared at the same consistencies as those for the tests with the fabric-covered wheel are shown in figs. 16-19. The following observations, generally parallel to those

given for the fabric-covered wheel, are made:

- a. The rate of increase in torque coefficient with slip, in the 0-20% slip range, tended to increase with soil strength, and the point at which the slope of the torque-slip relation changed rapidly was reached at a lower slip on the stronger soils.
- b. Again, there was no clear-cut indication that performance was best at any particular load. The pull coefficient increased slightly throughout the 20-80% slip range.

Power number versus pull coefficient/slope-climbing ability

20. The relations of power number versus pull coefficient/slope-climbing ability for the four soil conditions are presented in figs. 20-23. The power requirement is higher in the loose, compactible material particularly the S_1 and C_0 soil condition. The open-mesh wheel begins to pick up soil at about 10-20% slip, particularly the loosest wet sand, and carry it inside the wheel; more and more soil is picked up as slip increases, so that at 80% slip on the C_0 soil condition, the wheel may be carrying as much as 25 lb of soil (see fig. 24). Fig. 25 shows the wheel at the design load operating on a C_0 soil condition and illustrates that there may be energy losses due to sand transportation.

21. The trapping and retention of sand within the wheel are tentatively attributed to cohesion or adhesion of the sand particles. Scientists at the lunar receiving laboratory found that the lunar soil particles tended to adhere one to another during sieving operations, and so be retained on sieves with openings much larger than the particle size. It seems probable, therefore, that the open-mesh wheel may experience the same problem during a lunar traverse.

Efficiency

22. The efficiency (η') of the wheel did not display an definite trends relatable to load, but the average values for a given soil condition showed a systematic increase in efficiency with soil strength. The total increase over the range was 30%. This trend is in line with the assumption that motion resistance due to soil deformation increases as the soil strength decreases.

Sinkage

23. The relation of sinkage to slip for the soil condition with the smallest penetration resistance, C_0 , is shown in fig. 26. The load for this test was 59 lb.

Comparative Performance of Covered and Open Wheels

24. Contact pressure, wheel deformation, and tire print data measured on an unyielding surface at loads representing 50, 75, 100, 125, and 150% of the design load are listed in table 4 for both wheels.

Pull and torque

25. In general, the covered wheel developed higher pull and torque at a given slip level and a higher maximum pull than did the open wheel. Both wheels show the same trends toward variations in performance with load and soil strength.

Power number versus pull coefficient/slope-climbing ability

26. The power requirements of the two wheels at the self-propelled point on a level surface were not appreciably different. The data in tables 2 and 3 and the graphic displays indicate that the covered wheel may be able to negotiate slopes of 25 deg or greater in the denser soils

(with some cohesion), while the open-mesh wheel may not. Maximum slope-climbing ability of the open-mesh wheel is estimated at approximately 20 deg.

Efficiency

27. On the average, efficiencies at the 20% slip level were about the same for both wheels, and both wheels developed the poorest efficiency on the loose, wet sand (C_0) soil condition. That the efficiency of the covered wheel may be considerably greater at higher slips is indicated in a comparison of the data shown in figs. 27 and 28; that is, the spread between the torque-slip and pull-slip curves for a given pass is lower for the covered wheel at slips greater than about 35%.

Sinkage

28. It can be noted in figs. 15 and 26 that the sinkage for the open-mesh wheel was generally larger than that of the covered wheel; in fact, it was about twice as large.

Repetitive traffic

29. From visual observation, it was judged that the covered wheel compacts the soil more than the open-mesh wheel does, and thus leaves a firmer material in the path over which succeeding wheels travel. That is; the covered wheel's performance is improved on the second and third passes (the pull coefficient increases with each pass), as shown in fig. 27. The pull coefficient for the open-mesh wheel (fig. 28) shows no definite tendency to be altered by traffic. The torque coefficient for the open-mesh wheel begins to increase rapidly at slips greater than about 35%. This increase is tentatively attributed to the large amount of sand being thrown by the wheel and carried within it.

PART IV: CONCLUSIONS

30. The data collected and analyzed thus far are considered adequate to form the following tentative conclusions:

- a. The covered wheel had greater traction and slope-climbing ability.
- b. Power consumption rates (whr/km) were not greatly different for the two wheels on level surfaces and slopes of 15 deg or less.
- c. Present trends in the analysis indicate that power efficiency may be much lower for the open-mesh wheel than for the covered wheel at slips greater than 55 percent.
- d. In general, the data indicate that the wheels did not perform any better at one load than at another.
- e. On the C_0 soil condition, the covered wheel showed a tendency to improve performance on the second and third passes in the same path, whereas the open-mesh wheel did not.

Table 1. Soil Test Results (Before Traffic)

| Test No | Soil Condition | G pci | w % | D _r % | Y _d pcf | k _c | | n | φ _b deg | φ _{pl} deg | φ _t deg | c _b psi | c _{tr} psi |
|-----------------------|----------------|-------|-----|------------------|--------------------|----------------|--------------|------|--------------------|---------------------|--------------------|--------------------|---------------------|
| | | | | | | lb/in. (1tn) | lb/in. (2tn) | | | | | | |
| GM VII (Closed Wheel) | | | | | | | | | | | | | |
| 110 | S ₁ | 1.9 | 0.5 | 31 | 93.01 | -0.27 | 4.66 | 0.85 | 13.5 | 29.9 | 37.0 | 0.22 | 0 |
| 111 | S ₁ | 2.0 | 0.5 | 32 | 94.38 | 2.94 | 6.00 | 0.70 | 15.5 | 30.0 | 37.1 | 0.17 | 0 |
| 112 | S ₁ | 2.1 | 0.5 | 34 | 94.68 | 0.62 | 6.06 | 0.64 | 10.5 | 30.1 | 37.2 | 0.32 | 0 |
| 108 | C ₀ | 0.7 | 1.4 | (0) | 83.18 | 6.21 | 1.60 | 0.67 | 20.0 | 28.1 | 34.6 | 0 | 0.04 |
| 115 | C ₀ | 0.7 | 1.4 | (0) | 83.40 | 1.47 | 2.92 | 0.70 | 18.0 | 28.1 | 34.6 | 0.23 | 0.04 |
| 113 | C ₀ | 0.9 | 1.4 | (0) | 84.17 | 4.03 | 2.90 | 0.69 | 15.5 | 28.1 | 34.6 | 0.15 | 0.04 |
| 118 | C ₁ | 4.9 | 1.4 | 15 | 84.26 | -2.07 | 11.20 | 0.52 | 24.5 | 29.1 | 36.1 | 0.15 | 0.09 |
| 117 | C ₁ | 5.0 | 1.4 | 17 | 86.07 | -1.44 | 10.83 | 0.53 | 21.0 | 29.2 | 36.2 | 0.12 | 0.09 |
| 119 | C ₁ | 4.7 | 1.4 | 14 | 86.28 | -1.27 | 10.10 | 0.53 | 23.5 | 29.0 | 36.0 | 0.17 | 0.08 |
| 109 | C ₂ | 12.7 | 1.3 | 60 | 91.75 | 0.19 | 14.54 | 0.57 | 22.0 | 31.7 | 39.0 | 0.10 | 0.15 |
| 116 | C ₂ | 11.0 | 1.4 | 50 | 91.63 | 6.09 | 9.24 | 0.49 | 14.5 | 31.1 | 38.3 | 0.36 | 0.15 |
| 114 | C ₂ | 13.0 | 1.5 | 55 | 89.44 | 6.33 | 9.78 | 0.47 | 23.5 | 31.4 | 38.6 | 0.07 | 0.19 |
| GM VIII (Open Wheel) | | | | | | | | | | | | | |
| 9 | S ₁ | 2.0 | 0.5 | 32 | 94.35 | -0.48 | 8.08 | 0.77 | 11.5 | 30.0 | 37.1 | 0.28 | 0 |
| 8 | S ₁ | 1.8 | 0.5 | 29 | 95.48 | -0.22 | 5.53 | 0.74 | 22.0 | 28.9 | 36.9 | 0.10 | 0 |
| 10 | S ₁ | 2.0 | 0.5 | 32 | 94.78 | 0.64 | 5.74 | 0.67 | 9.0 | 30.0 | 37.1 | 0.35 | 0 |
| | C ₀ | 0.9 | 1.3 | (0) | 82.41 | 1.48 | 2.29 | 0.71 | 15.0 | 28.1 | 34.6 | 0.22 | 0.03 |
| | C ₀ | 0.7 | 1.3 | (0) | 81.91 | 0.71 | 2.55 | 0.86 | 27.0 | 28.1 | 34.6 | 0.06 | 0.03 |
| 4 | C ₀ | 0.8 | 1.4 | (0) | 80.49 | 1.78 | 2.52 | 0.79 | 32.0 | 28.1 | 34.6 | 0.03 | 0.04 |

(Continued)

Table 1 (Concluded)

| Test No | Soil Condition | G pcf | w % | $\frac{D_r}{Z}$ | γ_d pcf | k_c lb/in. (1+ π) | k_ϕ lb/in. (2+ π) | n | ϕ_b deg | ϕ_{pl} deg | ϕ_t deg | c_b psi | c_{tr} psi |
|---------|----------------|-------|-----|-----------------|----------------|--------------------------|-----------------------------|------|--------------|-----------------|--------------|-----------|--------------|
| 12 | C ₁ | 4.3 | 1.4 | 9 | 84.76 | 2.23 | 5.03 | 0.65 | 18.0 | 28.6 | 35.7 | 0.29 | 0.07 |
| 3 | C ₁ | 4.7 | 1.3 | 17 | 86.36 | 1.95 | 5.32 | 0.71 | 30.0 | 29.2 | 36.2 | 0.12 | 0.07 |
| 5 | C ₁ | 4.3 | 1.3 | 13 | 87.70 | 1.87 | 5.69 | 0.66 | 23.5 | 28.9 | 36.0 | 0 | 0.07 |
| 13 | C ₂ | 11.1 | 1.4 | 51 | 91.64 | 3.01 | 10.38 | 0.54 | 10.0 | 31.0 | 38.4 | 0.35 | 0.15 |
| 2 | C ₂ | 10.8 | 1.4 | 49 | 90.30 | 7.79 | 7.40 | 0.54 | 9.0 | 31.0 | 38.1 | 0.52 | 0.15 |
| 11 | C ₂ | 11.4 | 1.6 | 45 | 91.70 | 6.40 | 9.13 | 0.53 | 11.5 | 30.7 | 37.8 | 0.44 | 0.19 |

Table 2. Results of Tests with the CM VII (Covered) Wheel

| Test No. | Soil Condition | G | | Load W N lb | Contact Pressure p _c | | P ₂₀ /W M/W | M ₂₀ /W M/W | n ₂₀ ^o | PN _{sp} [*] | PN _{max} ^{**} | PN ₁₅ [†] | PN ₂₅ [†] | |
|--------------------|----------------|-------------------|------|----------------|---------------------------------|-----|---------------------------|---------------------------|------------------------------|-------------------------------|---------------------------------|-------------------------------|-------------------------------|------|
| | | MN/m ³ | pci | | kN/m ² | psi | | | | | | | | |
| 69-110 | S ₁ | 0.52 | 1.9 | 195 | 44 | 6.9 | 1.00 | 0.37 | 0.54 | 0.55 | 0.12 | 0.62 | 0.47 | ∞ |
| -111 | S ₁ | 0.54 | 2.0 | 260 | 59 | 7.3 | 1.06 | 0.39 | 0.54 | 0.58 | 0.10 | 0.58 | 0.46 | ∞ |
| -112 | S ₁ | 0.57 | 2.1 | 325 | 73 | 7.7 | 1.12 | 0.36 | 0.53 | 0.54 | 0.16 | 0.70 | 0.55 | ∞ |
| -108 | C ₀ | 0.19 | 0.7 | 195 | 44 | 6.9 | 1.00 | 0.33 | 0.52 | 0.51 | 0.04 | 0.74 | 0.50 | ∞ |
| -115 | C ₀ | 0.20 | 0.7 | 260 | 59 | 7.3 | 1.06 | 0.36 | 0.55 | 0.52 | 0.14 | 0.78 | 0.54 | ∞ |
| -113 | C ₀ | 0.23 | 0.9 | 325 | 73 | 7.7 | 1.12 | 0.36 | 0.57 | 0.51 | 0.18 | 0.66 | 0.50 | ∞ |
| -118 | C ₁ | 1.31 | 4.9 | 195 | 44 | 6.9 | 1.00 | 0.51 | 0.62 | 0.66 | 0.06 | 0.66 | 0.36 | 0.57 |
| -117 | C ₁ | 1.34 | 5.0 | 260 | 59 | 7.3 | 1.06 | 0.52 | 0.61 | 0.68 | 0.06 | 0.77 | 0.38 | 0.60 |
| -119 | C ₁ | 1.28 | 4.7 | 325 | 73 | 7.7 | 1.12 | 0.49 | 0.58 | 0.68 | 0.08 | 0.66 | 0.36 | 0.54 |
| -109 | C ₂ | 3.44 | 12.7 | 195 | 44 | 6.9 | 1.00 | 0.52 | 0.62 | 0.67 | 0.06 | 0.70 | 0.38 | 0.60 |
| -116 | C ₂ | 2.95 | 11.0 | 260 | 59 | 7.3 | 1.06 | 0.47 | 0.60 | 0.63 | 0.10 | 0.80 | 0.46 | 0.72 |
| -114 | C ₂ | 3.50 | 13.0 | 325 | 73 | 7.7 | 1.12 | 0.49 | 0.63 | 0.62 | 0.10 | 0.76 | 0.43 | 0.65 |
| <u>Second Pass</u> | | | | | | | | | | | | | | |
| -115 | C ₀ | 0.78 | 2.9 | 260 | 59 | 7.3 | 1.06 | 0.48 | 0.61 | 0.63 | 0.12 | 0.81 | 0.50 | 0.78 |
| <u>Third Pass</u> | | | | | | | | | | | | | | |
| -115 | C ₀ | 0.74 | 2.7 | 260 | 59 | 7.3 | 1.06 | 0.50 | 0.61 | 0.66 | 0.06 | 0.73 | 0.43 | 0.69 |

* Power number at self-propelled point.

** Power number at point where the rate of increase in power number rapidly increases.

† Power numbers for 15- and 25-deg slopes, respectively (∞ denotes inability to climb).

NOTE: To compute power consumption rate (PCR) in whr/km/wheel on a given slope, e.g. 15 deg, calculate:

$$PCR = PN_{15} \times \frac{1000}{3600} \times \text{wheel load (in newtons)}$$

Table 3. Results of Tests with the GM VIII (Open) Wheel

| Test No. | Soil Condition | $\frac{G}{MN/m^3}$ | $\frac{Load}{N}$ | $\frac{W}{lb}$ | Contact Pressure | | $\frac{P_{20}/W}{M_{20}/W}$ | $\frac{n'_{20}}{n_{20}}$ | $\frac{PN^*}{sp}$ | $\frac{PN^{**}}{max}$ | $\frac{PN^\dagger}{15}$ | $\frac{PN^\ddagger}{25}$ | | |
|--------------------|----------------|--------------------|------------------|----------------|----------------------|-------------------|-----------------------------|--------------------------|-------------------|-----------------------|-------------------------|--------------------------|------|-----|
| | | | | | $\frac{kN/m^2}{psi}$ | $\frac{sure}{pc}$ | | | | | | | | |
| <u>First Pass</u> | | | | | | | | | | | | | | |
| 9 | S ₁ | 0.55 | 2.1 | 195 | 44 | 6.9 | 1.00 | 0.32 | 0.50 | 0.51 | 0.10 | 0.48 | 0.41 | ∞ |
| 8 | S ₁ | 0.48 | 1.8 | 260 | 59 | 7.3 | 1.06 | 0.35 | 0.48 | 0.58 | 0.08 | 0.56 | 0.42 | ∞ |
| 10 | S ₁ | 0.53 | 2.0 | 325 | 73 | 7.7 | 1.12 | 0.35 | 0.45 | 0.62 | 0.08 | 0.55 | 0.44 | ∞ |
| 7 | C ₀ | 0.25 | 0.9 | 195 | 44 | 6.9 | 1.00 | 0.31 | 0.51 | 0.49 | 0.10 | 0.76 | 0.57 | ∞ |
| 1 | C ₀ | 0.20 | 0.7 | 260 | 59 | 7.3 | 1.06 | 0.38 | 0.57 | 0.53 | 0.08 | 0.64 | 0.45 | 2.8 |
| 4 | C ₀ | 0.21 | 0.8 | 325 | 73 | 7.7 | 1.12 | 0.30 | 0.51 | 0.47 | 0.14 | 0.53 | 0.44 | ∞ |
| 12 | C ₁ | 1.16 | 4.3 | 195 | 44 | 6.9 | 1.00 | 0.39 | 0.47 | 0.66 | 0.09 | 0.45 | 0.33 | 2.1 |
| 3 | C ₁ | 1.26 | 4.7 | 260 | 59 | 7.3 | 1.06 | 0.34 | 0.47 | 0.58 | 0.12 | 0.52 | 0.40 | ∞ |
| 5 | C ₁ | 1.15 | 4.3 | 325 | 73 | 7.7 | 1.12 | 0.37 | 0.48 | 0.62 | 0.10 | 0.46 | 0.35 | ∞ |
| 13 | C ₂ | 3.02 | 11.3 | 195 | 44 | 6.9 | 1.00 | 0.37 | 0.48 | 0.62 | 0.06 | 0.57 | 0.39 | ∞ |
| 2 | C ₂ | 2.91 | 10.8 | 260 | 59 | 7.3 | 1.06 | 0.37 | 0.46 | 0.64 | 0.09 | 0.53 | 0.38 | ∞ |
| 11 | C ₂ | 3.09 | 11.9 | 325 | 73 | 7.7 | 1.12 | 0.36 | 0.41 | 0.70 | 0.07 | 0.49 | 0.34 | ∞ |
| <u>Second Pass</u> | | | | | | | | | | | | | | |
| 70-1 | C ₀ | 0.66 | 2.4 | 260 | 59 | 7.3 | 1.06 | 0.43 | 0.51 | 0.67 | 0.03 | 0.61 | 0.39 | 2.0 |
| <u>Third Pass</u> | | | | | | | | | | | | | | |
| 70-1 | C ₀ | 0.71 | 2.6 | 260 | 59 | 7.3 | 1.06 | 0.37 | 0.49 | 0.60 | 0.11 | 0.61 | 0.45 | ∞ |

* Power number at self-propelled point.

** Power number at point where the rate of increase in power number rapidly increases.

† Power numbers for P/W = 0.27 and 0.47, respectively (∞ denotes inability to climb).

NOTE: To compute power consumption rate (PCR) in whr/km/wheel on a given slope, e.g. 15 deg calculate:

$$PCR = PN_{15} \times \frac{1000}{3600} \times \text{wheel load (in newtons)}$$

Table 4. Tire Data*

| Deflection Computed in. | Load % ^{***} lb | Carcass Diam- eter in. | Section Height in. | | Section Width in. | Measured Rolling Circum- ference ft | Contact Area sq in. | Tire Print in. | | Contact Pressure psi |
|-------------------------------|--------------------------------|---------------------------------|--------------------------|----------|-------------------------|---|---------------------------|-------------------|-------|----------------------------|
| | | | Loaded | Unloaded | | | | Length | Width | |
| | | | | | | | | | | |
| <u>GM VII (Closed) Wheel</u> | | | | | | | | | | |
| 0.85 | 5.3 | 29.23 | 6.44 | 7.29 | 9.90 | 9.45 | 32.97 | 7.45 | 5.30 | 0.90 |
| 1.19 | 7.4 | 43.84 | 6.11 | 7.29 | 10.10 | 9.45 | 44.12 | 9.03 | 6.23 | 1.00 |
| 1.46 | 9.1 | 58.45 | 5.83 | 7.24 | 10.43 | 9.45 | 55.26 | 9.82 | 6.85 | 1.06 |
| 1.76 | 11.0 | 73.07 | 5.53 | 7.29 | 10.74 | 9.45 | 65.84 | 10.58 | 7.40 | 1.12 |
| 2.10 | 13.1 | 87.68 | 5.19 | 7.29 | 11.15 | 9.45 | 71.14 | 10.95 | 7.93 | 1.23 |
| <u>GM VIII (Open) Wheel</u> | | | | | | | | | | |
| 1.23 | 7.6 | 29.23 | 6.21 | 7.44 | 10.00 | 9.15 | 54.87 | 10.08 | 6.58 | 0.54 |
| 1.66 | 10.3 | 43.84 | 5.79 | 7.44 | 10.36 | 9.15 | 59.80- | 10.73 | 6.44 | 0.74 |
| 2.11 | 13.0 | 58.45 | 5.34 | 7.44 | 10.72 | 9.15 | 76.57 | 11.75 | 7.74 | 0.77 |
| 2.37 | 14.7 | 73.07 | 5.08 | 7.44 | 11.10 | 9.15 | 90.60 | 12.15 | 8.80 | 0.81 |
| 3.62 | 16.2 | 87.68 | 4.83 | 7.44 | 11.52 | 9.15 | 101.84 | 13.25 | 9.13 | 0.87 |

* All data given represent an average of two measurements at diametrically opposite positions.

** Deflection % = $(2\delta/d) \times 100$.

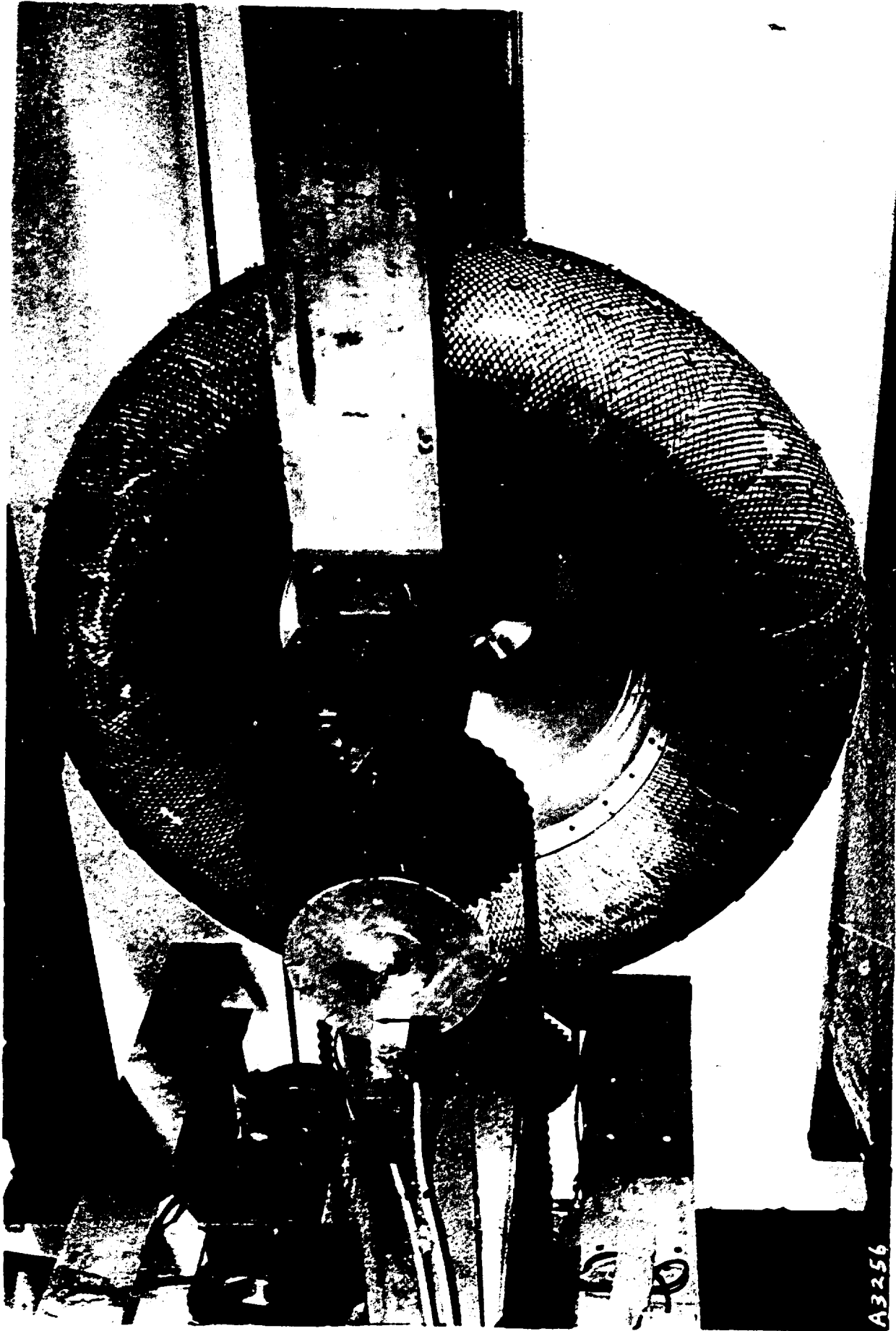


Fig. 1a. Fabric-covered wheel (GM VII)

A3256

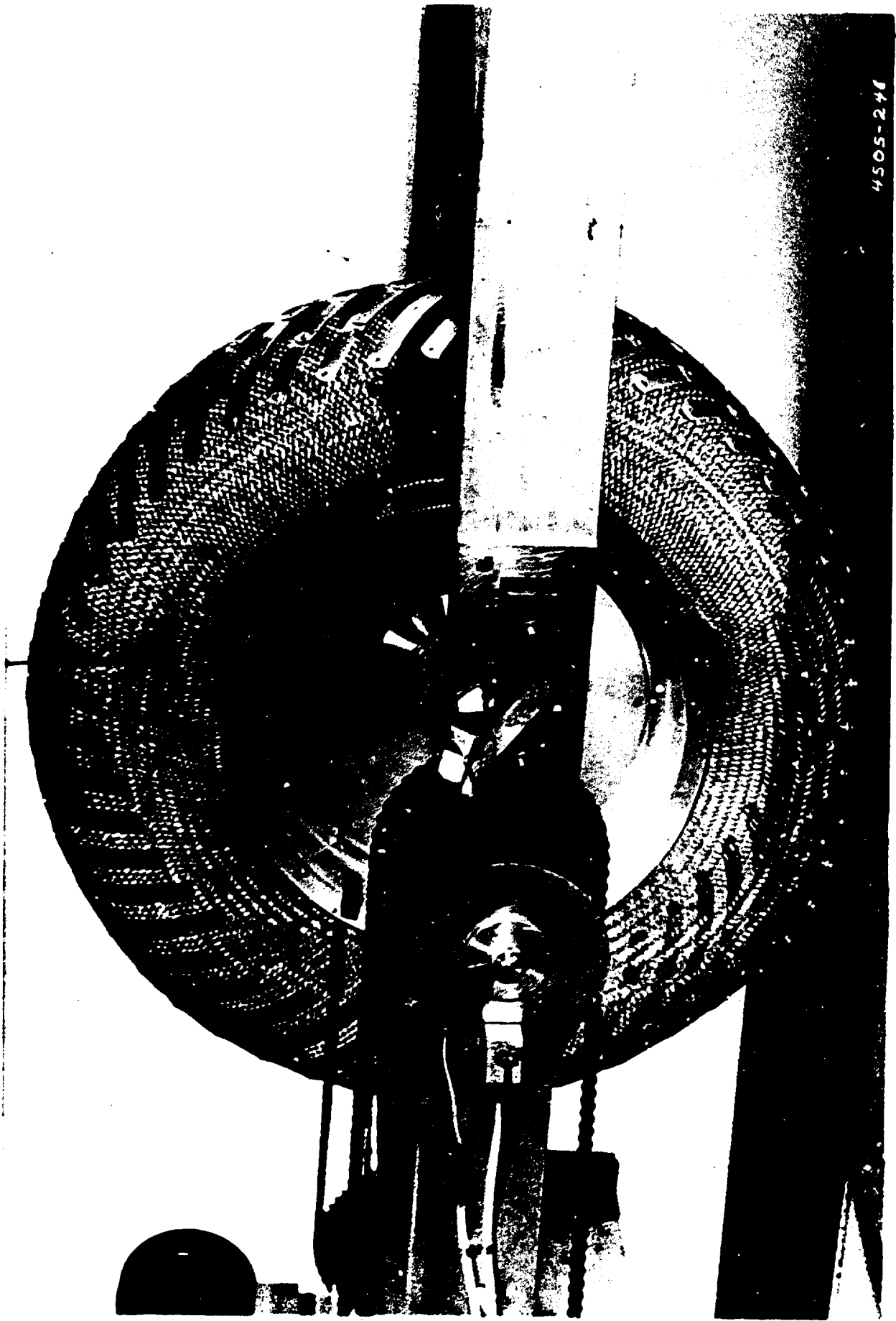
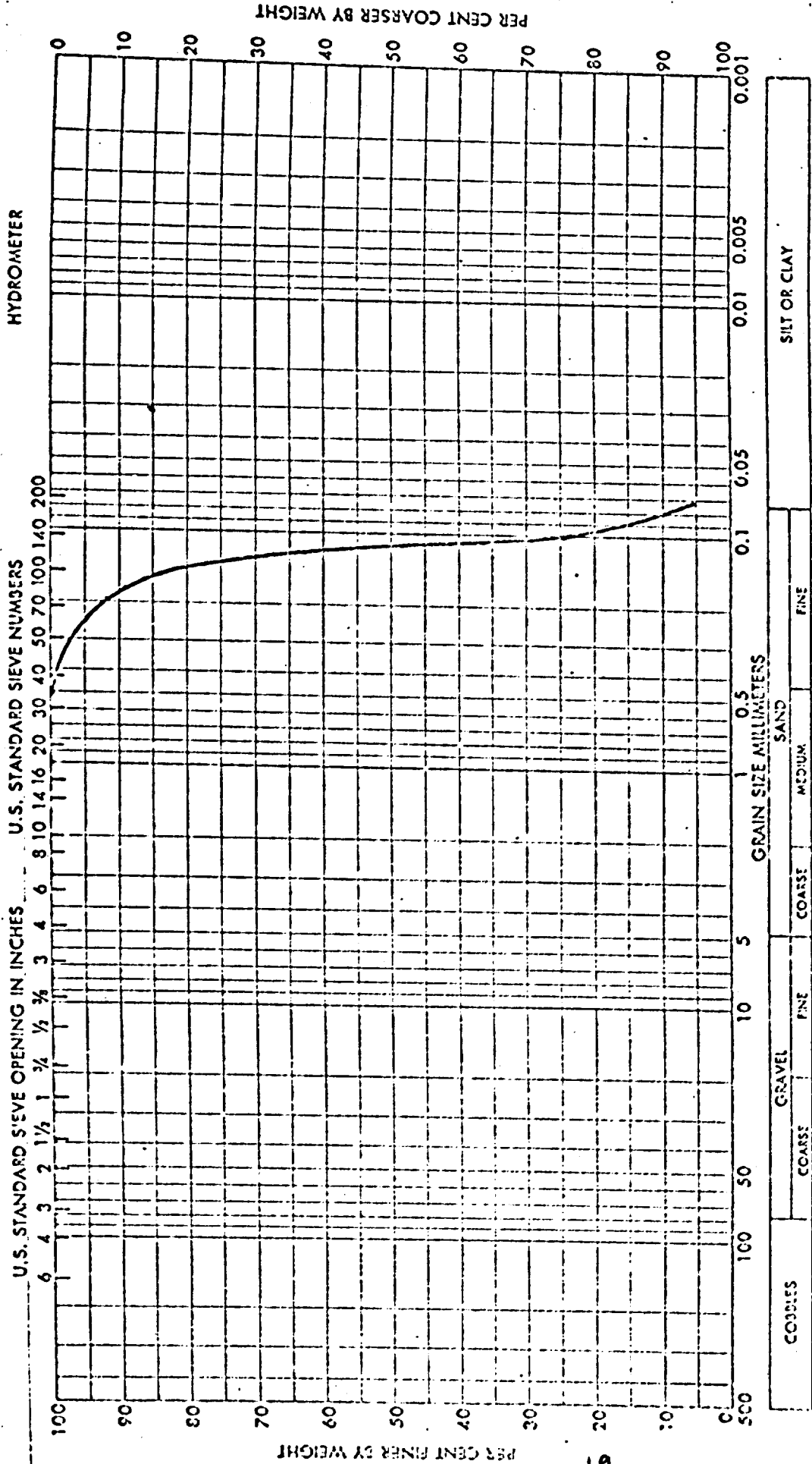


Fig. 1b. Open-weave wheel (CN VIII)

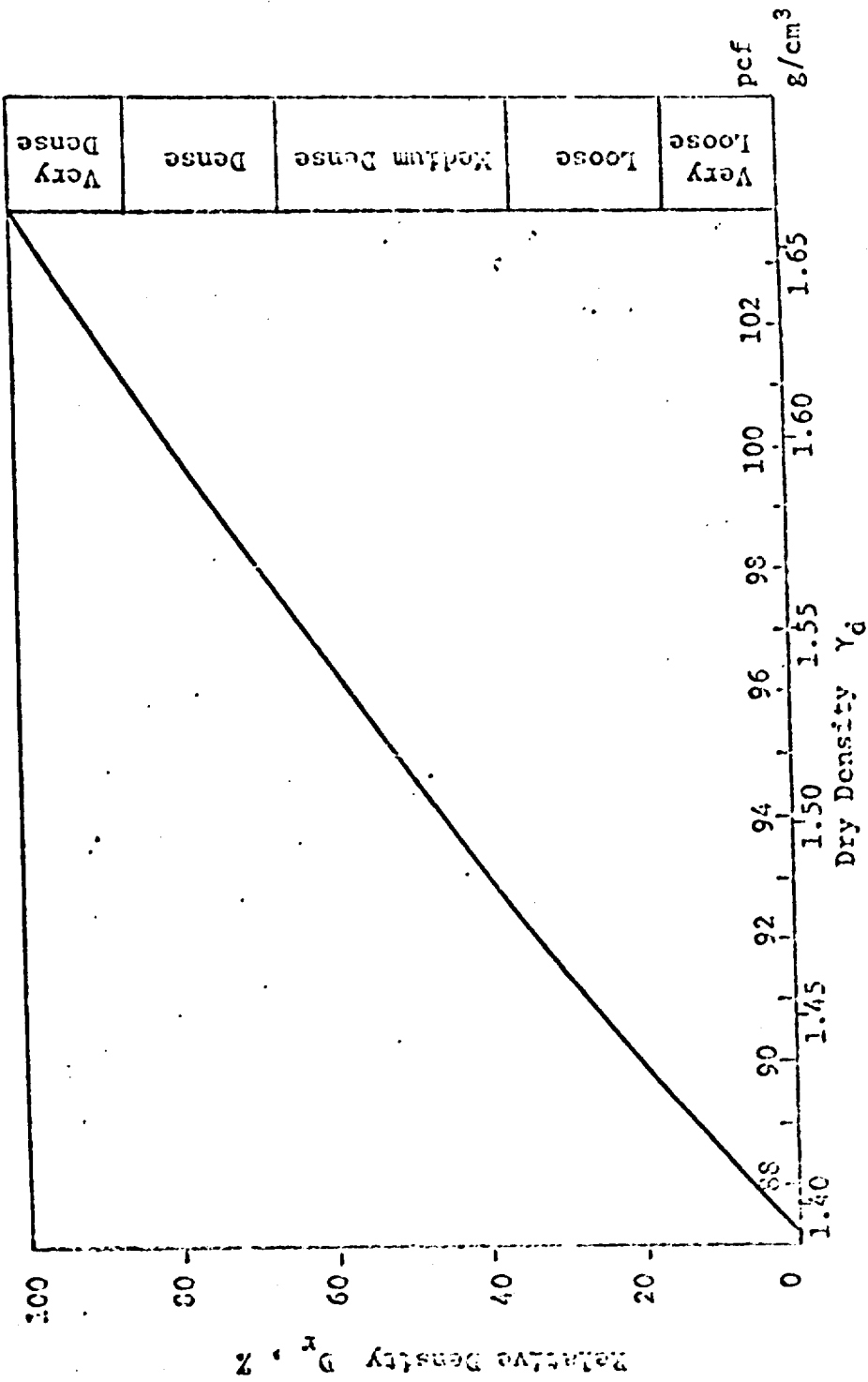


Soil Properties

$C_u = 1.5$ $d_m = 0.12 \text{ mm}$ $e_{min} = 0.608$ $D' = 51.2\%$

$\hat{c}_{50} = 0.12 \text{ mm}$ $e_{max} = 0.919$ $e_{max} - e_{min} = 0.311$ $\gamma_s = 2.67$

Fig. 2. Grain-size distribution and soil properties of Yuma sand



$Y_d \text{ min} = 1.39 \text{ g/cm}^3 \text{ (87 pcf)}$
 $Y_d \text{ max} = 1.66 \text{ g/cm}^3 \text{ (104 pcf)}$

Fig. 3. Relation between dry density Y_d and relative density D_r of Yuma sand

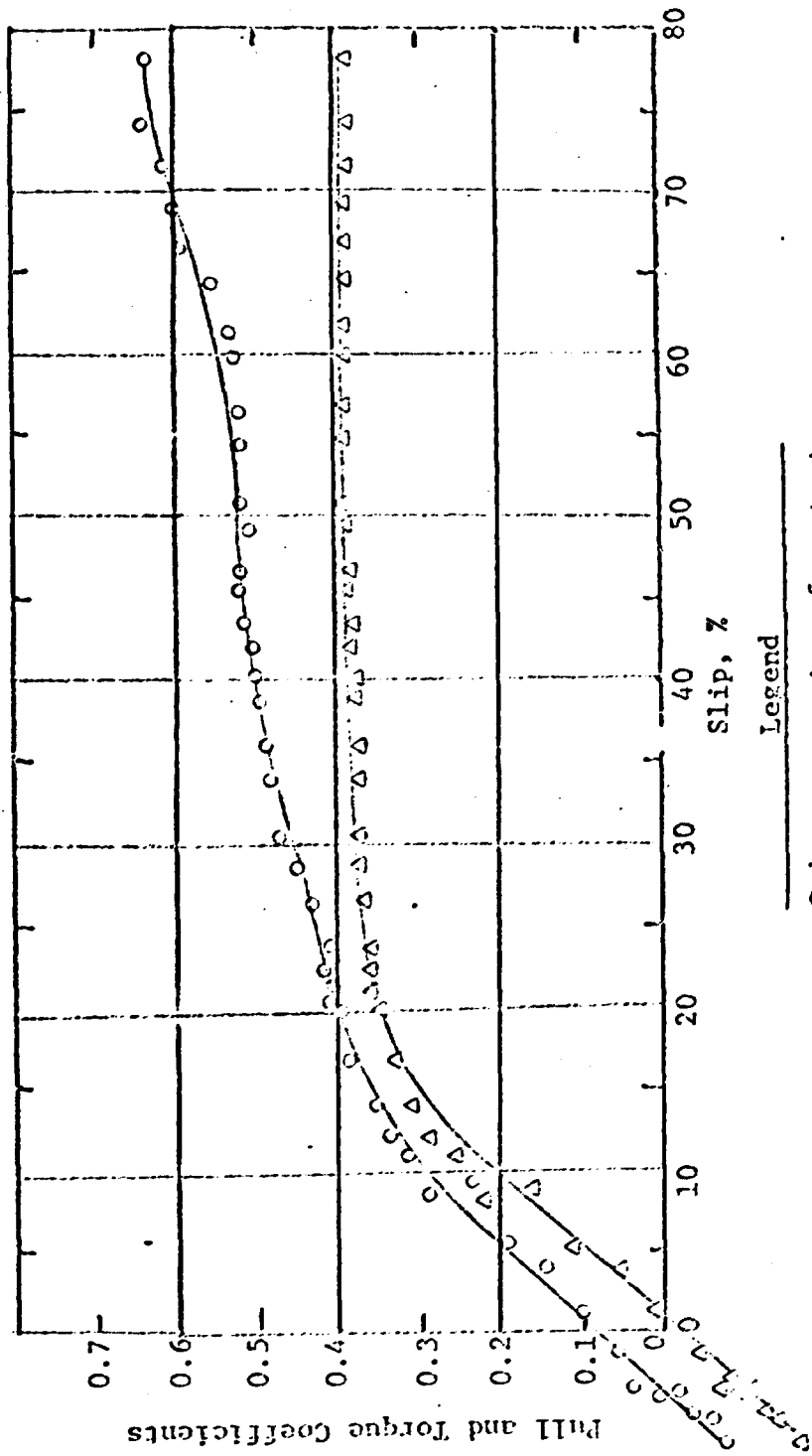


Fig. 4. Representative relations of pull and torque coefficients to slip for the open mesh wheel (GX VIII); wet sand C_1 ; $G \approx 4.9$ psi/in.; $c = 0.09$ psi; $w = 1.4\%$; Load = 59 lb

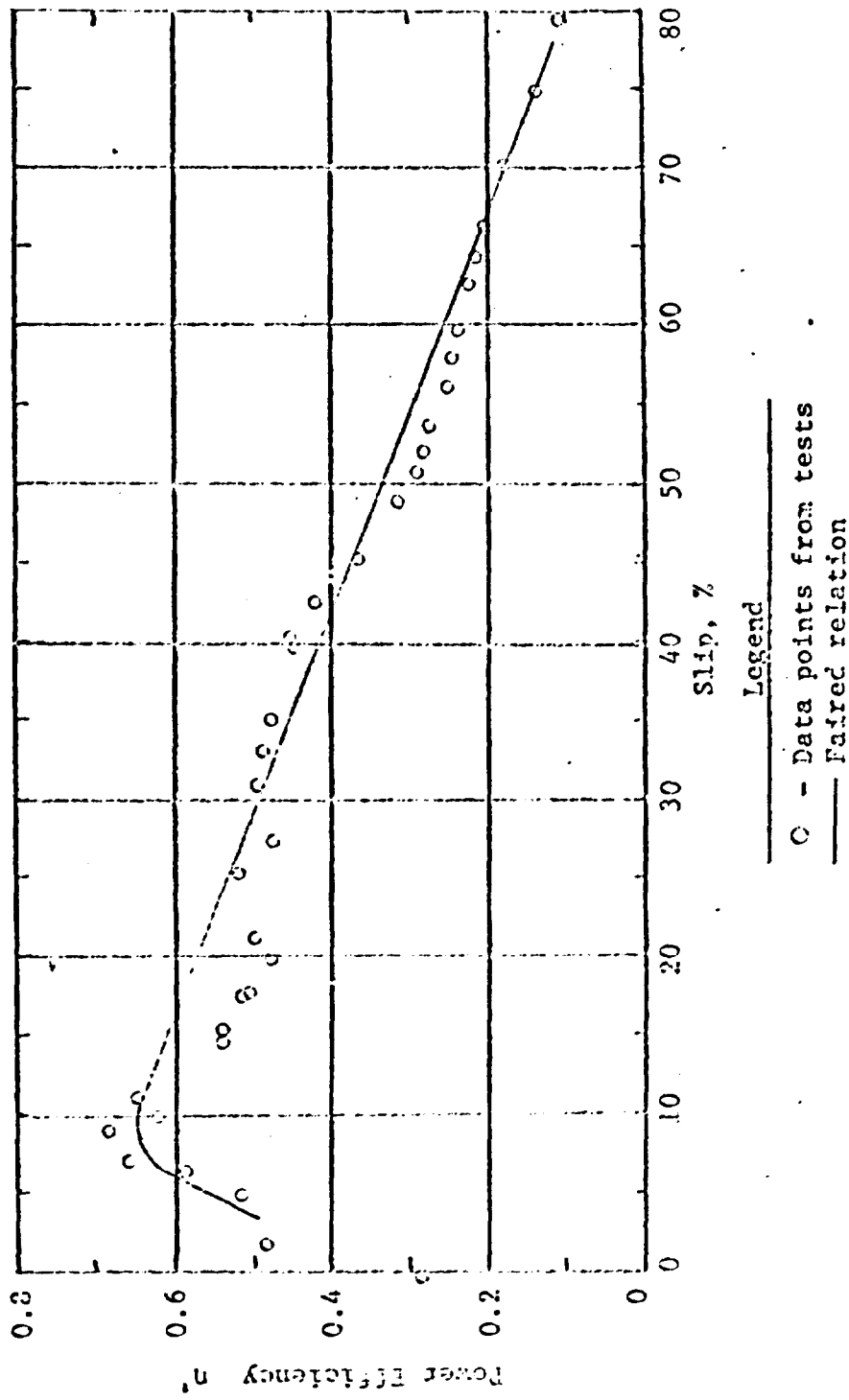


Fig. 5. Representative relations of power efficiency to slip for the open mesh wheel (GX VIII)
 Wet sand c_0 : $G \approx 0.8$ psi/in.; $c = 0.04$ psi; $w = 1.4\%$; load = 59 lb (260 N)

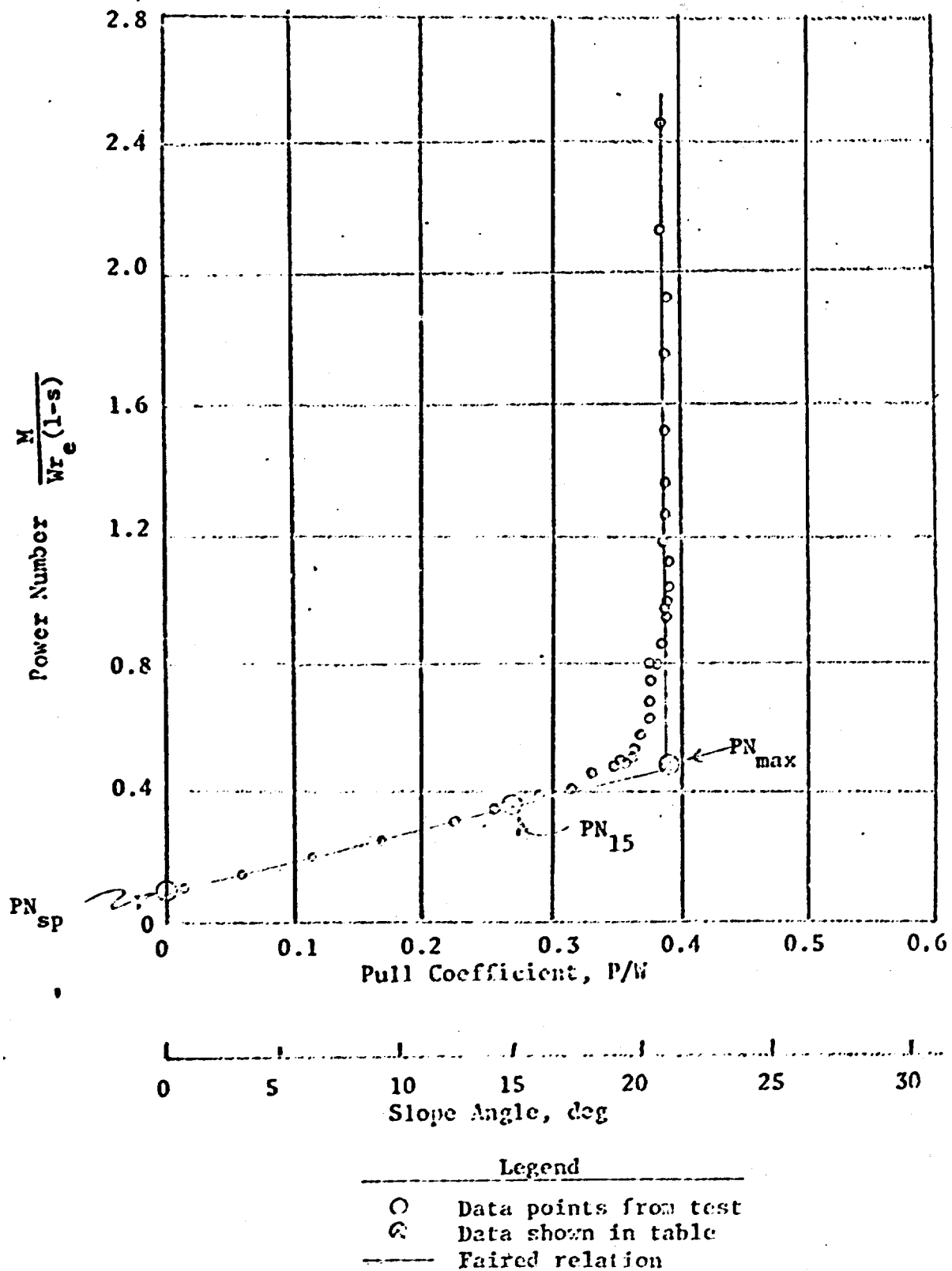


Fig. 6. Representative relations of power number to pull coefficient for the open mesh wheel (GM VIII); wet sand C_o ; $G \approx 0.8$ psi/in.; $c = 0.04$ psi; load = 59 lb (260 N)

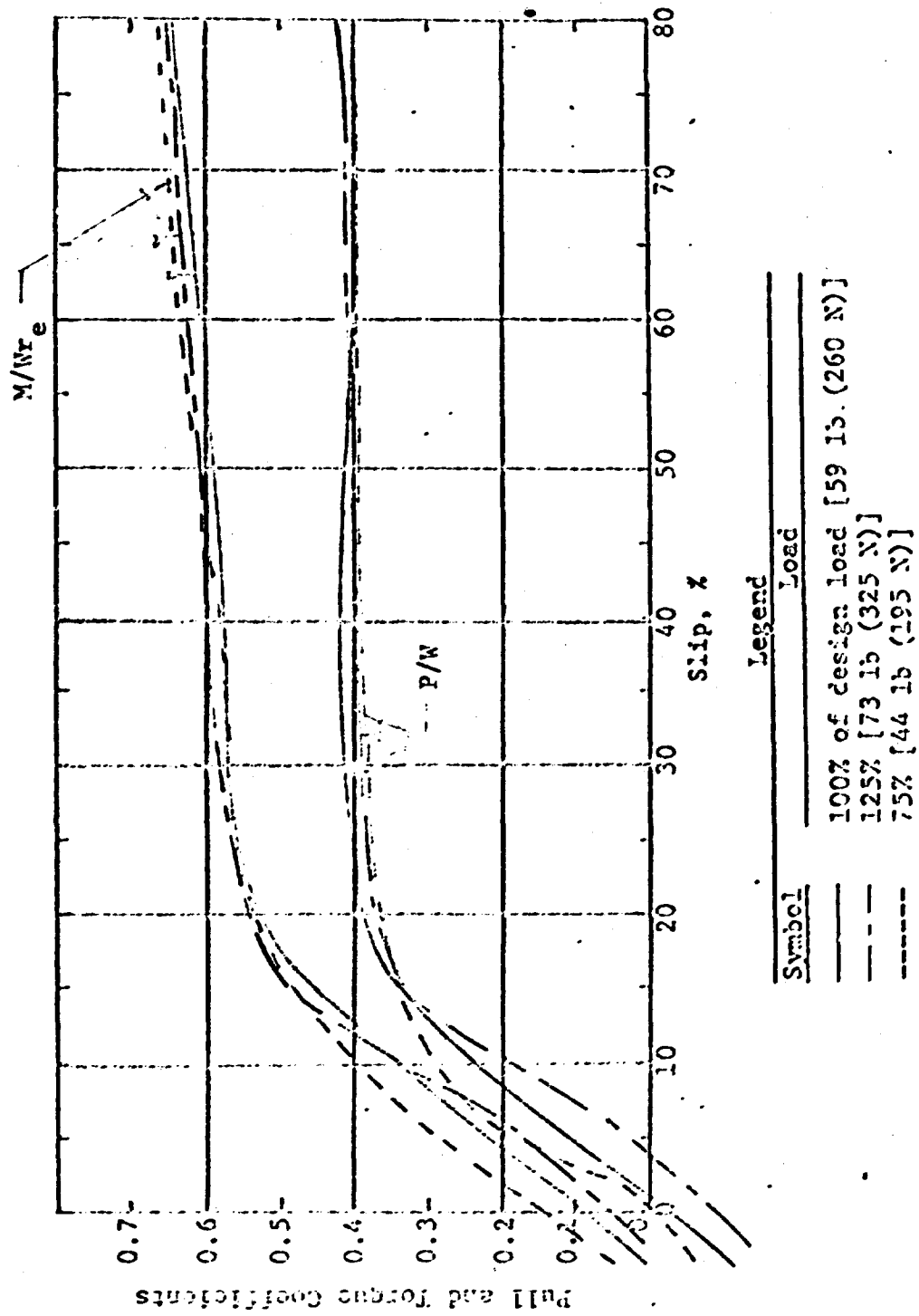


Fig. 7. Pull and torque coefficients versus slip for the fabric-covered wheel (GX VII);
 Air dry sand S_1 ; $G \approx 2.0$ psi/in.; $c = 0.0$ psi; $w = 1.5\%$

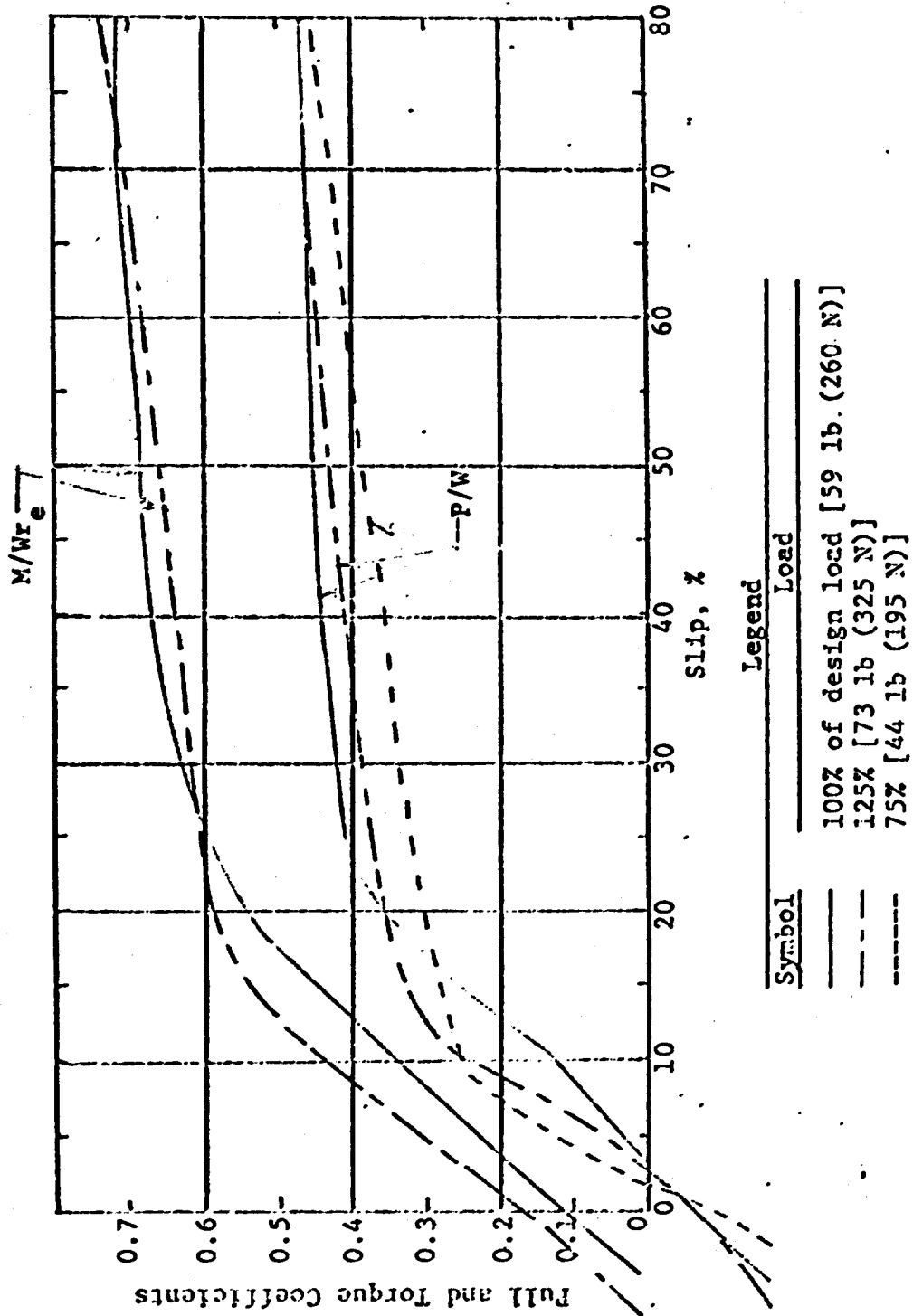


Fig. 8. Pull and torque coefficients versus slip for the fabric-covered (GM VIII); wet sand C_0 ; $G \approx 0.8$ psi/in.; $c = 0.04$ psi; $w = 1.4\%$

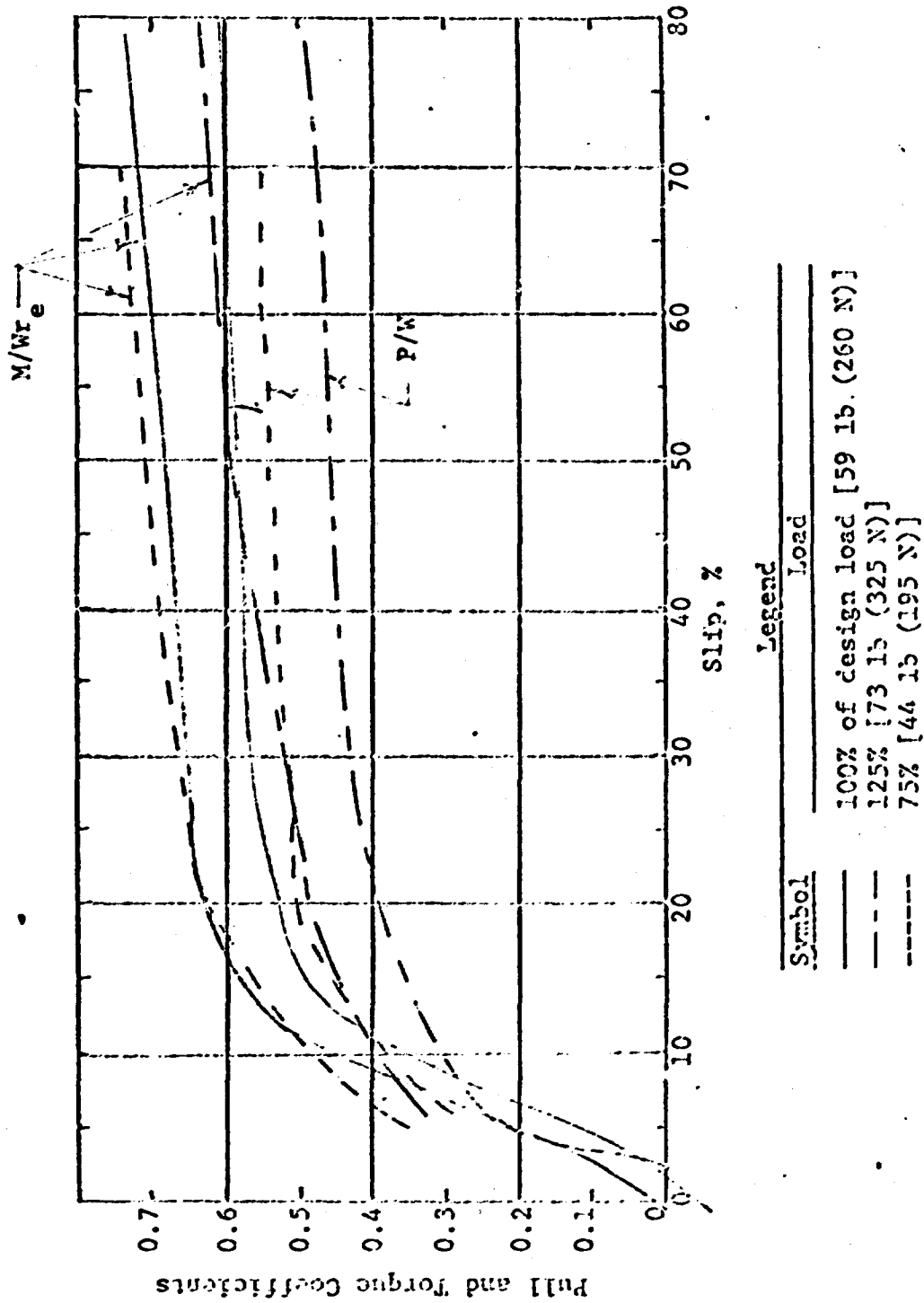


Fig. 9. Pull and torque coefficients versus slip for the fabric-covered wheel (GM VII); wet sand C_1' ; $C \approx 4.9$ psi/in.; $c = 0.09$ psi; $w = 1.4\%$

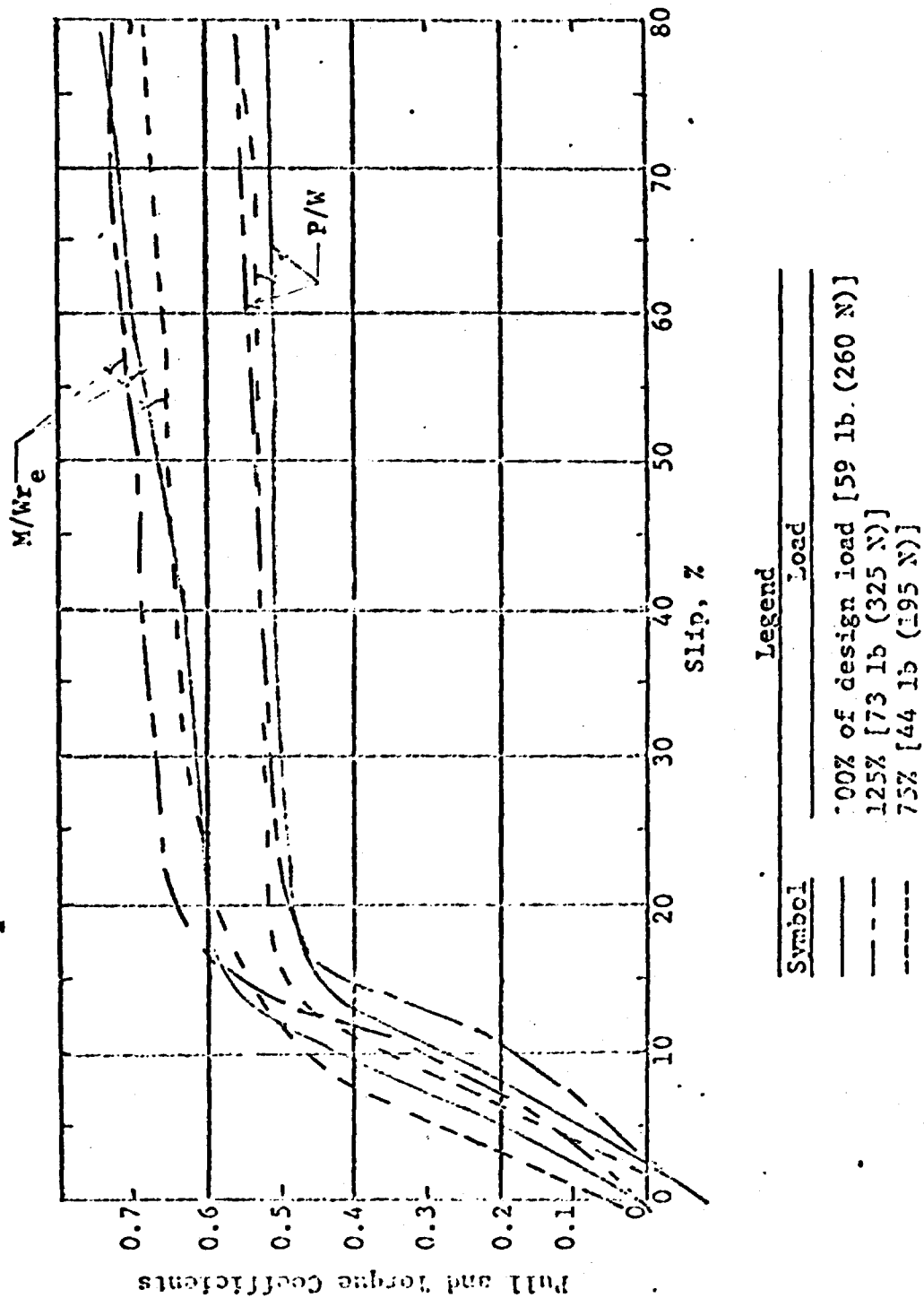
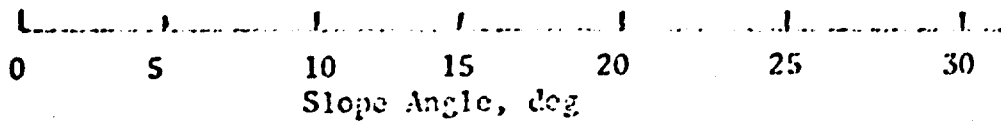
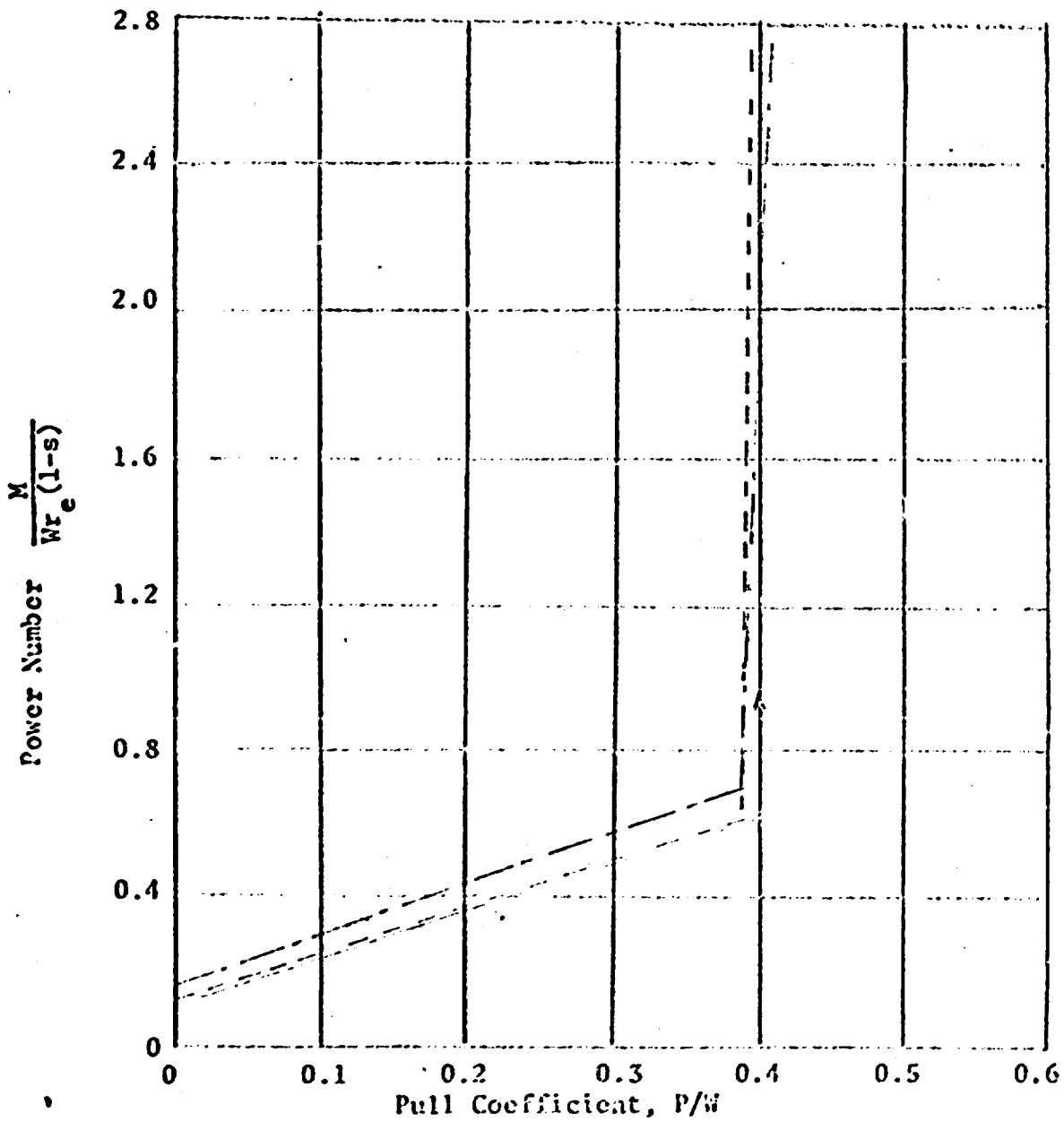
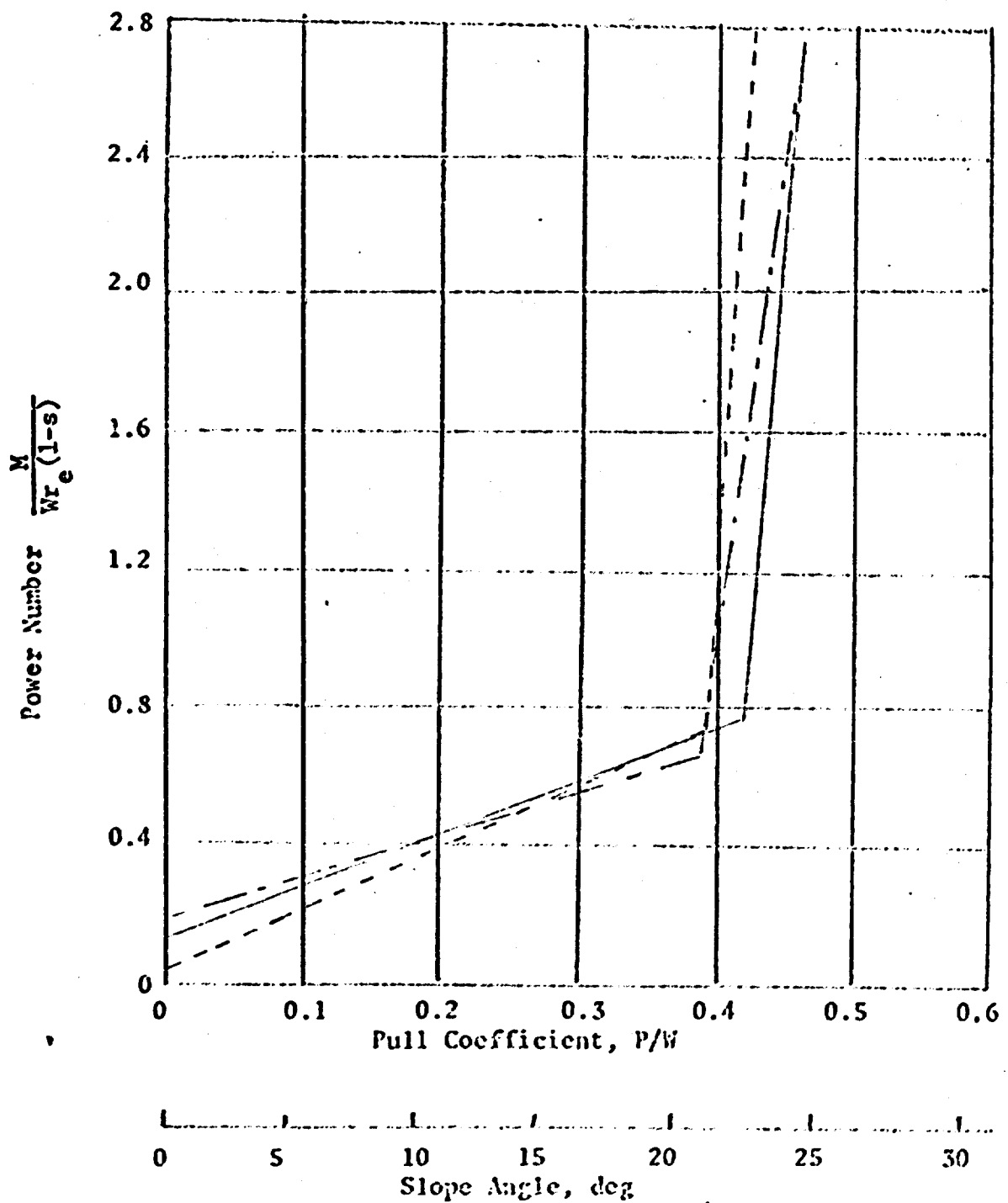


Fig. 10. Pull and torque coefficients versus slip for the fabric-covered wheel (GM VII): wet sand C_2 ; $G \approx 12.0$ psi/in.; $c = 0.16$ psi; $w = 1.4\%$



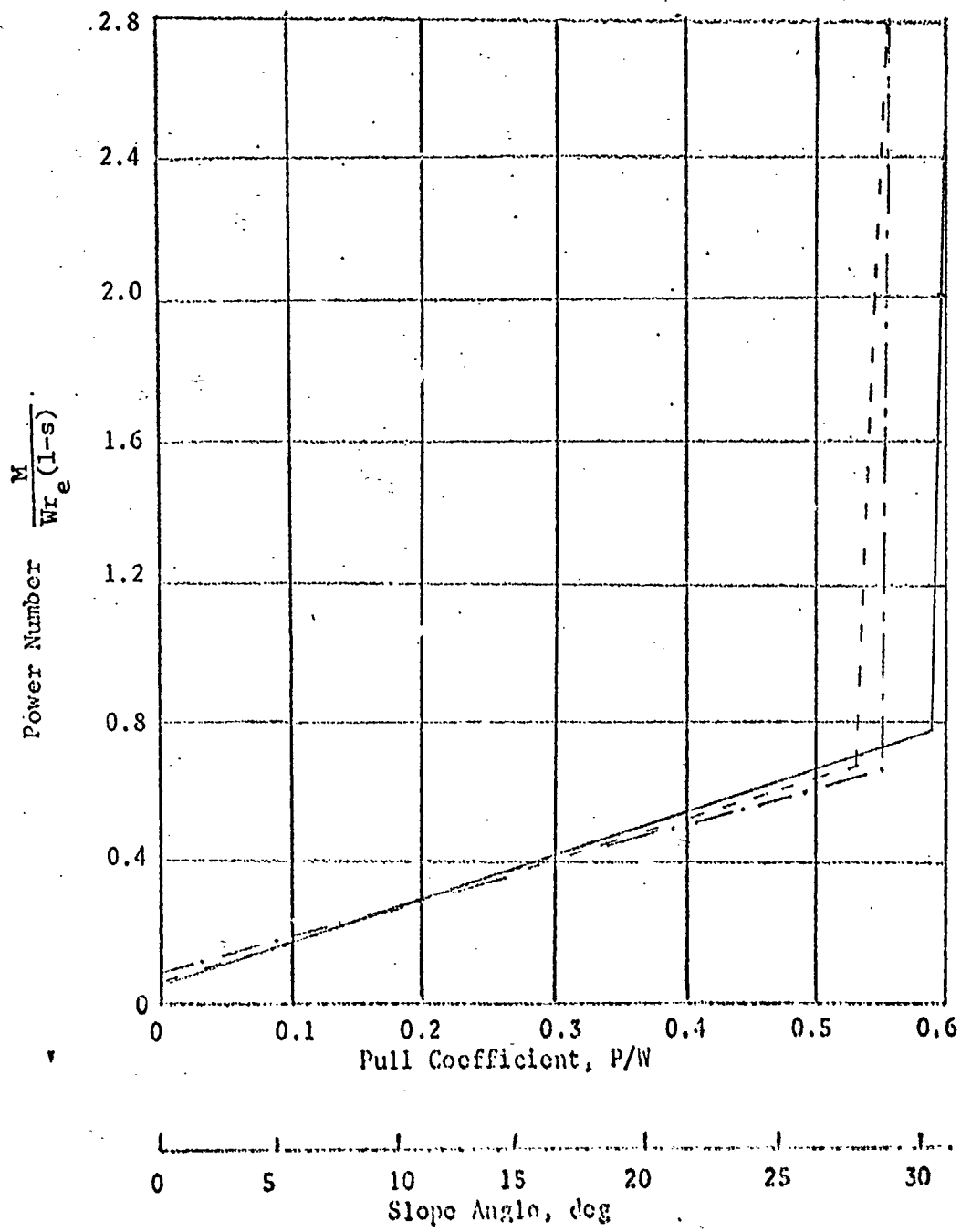
| Legend | |
|---------|-------------------------------------|
| Symbol | Load |
| — | 100% of design load [59 lb (260 N)] |
| - - - | 125% [73 lb (325 N)] |
| - · - · | 75% [44 lb (195 N)] |

Fig. 11. Power number versus pull coefficient for the fabric-covered wheel (CN VII) dry sand S_1 ; $G = 2$ psi/in.; $c = 0.0$ psi



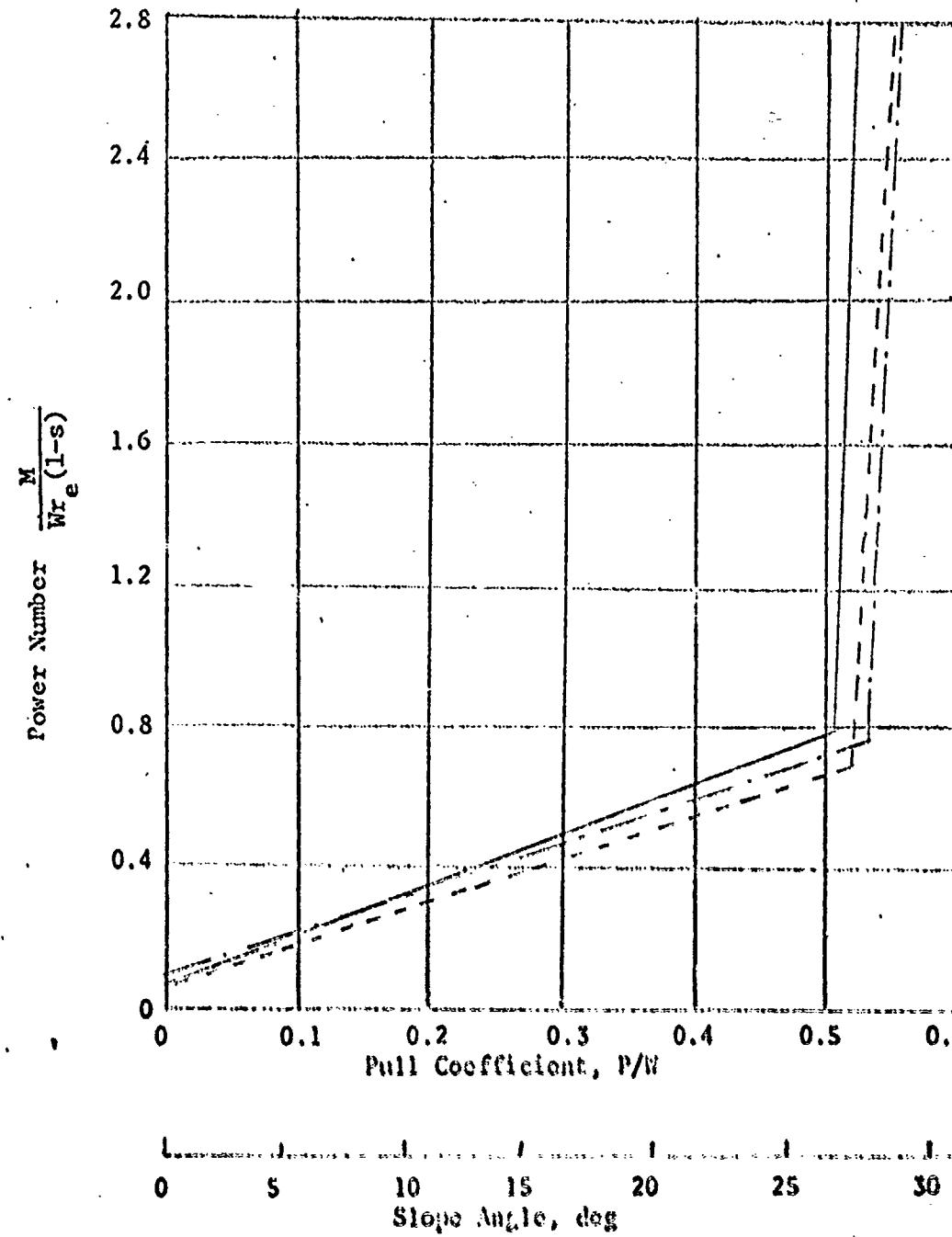
| Legend | |
|---------|-------------------------------------|
| Symbol | Load |
| — | 100% of design load [59 lb (260 N)] |
| - - - | 125% [73 lb (325 N)] |
| - · - · | 75% [44 lb (195 N)] |

Fig. 12. Power number versus pull coefficient for the fabric-covered wheel (G: V11); wet sand C_0 ; $G = 0.8$ psi/in.; $c = 0.04$ psi; $w = 1.47$



| Legend | |
|-----------|--------------------------------------|
| Symbol | Load |
| — | 100% of design load [59 lb. (260 N)] |
| - - - | 125% [73 lb (325 N)] |
| - · - · - | 75% [44 lb (195 N)] |

Fig. 13. Power number versus pull coefficient for the fabric-covered wheel (GM VII); wet sand G_1 ; $G = 4.9$ psi/in.; $c = 0.09$ psi; $w = 1.4X$



| Legend | |
|-----------|-------------------------------------|
| Symbol | Load |
| — | 100% of design load [59 lb (260 N)] |
| - - - | 125% [73 lb (325 N)] |
| - · - · - | 75% [44 lb (195 N)] |

Fig. 14. Power number versus pull coefficient for the fabric-covered wheel (W VII); wet sand C_2 ; $C = 12.0 \text{ psi/in.}$

$$c = 0.16 \text{ psi} \cdot \nu = 1.4\%$$

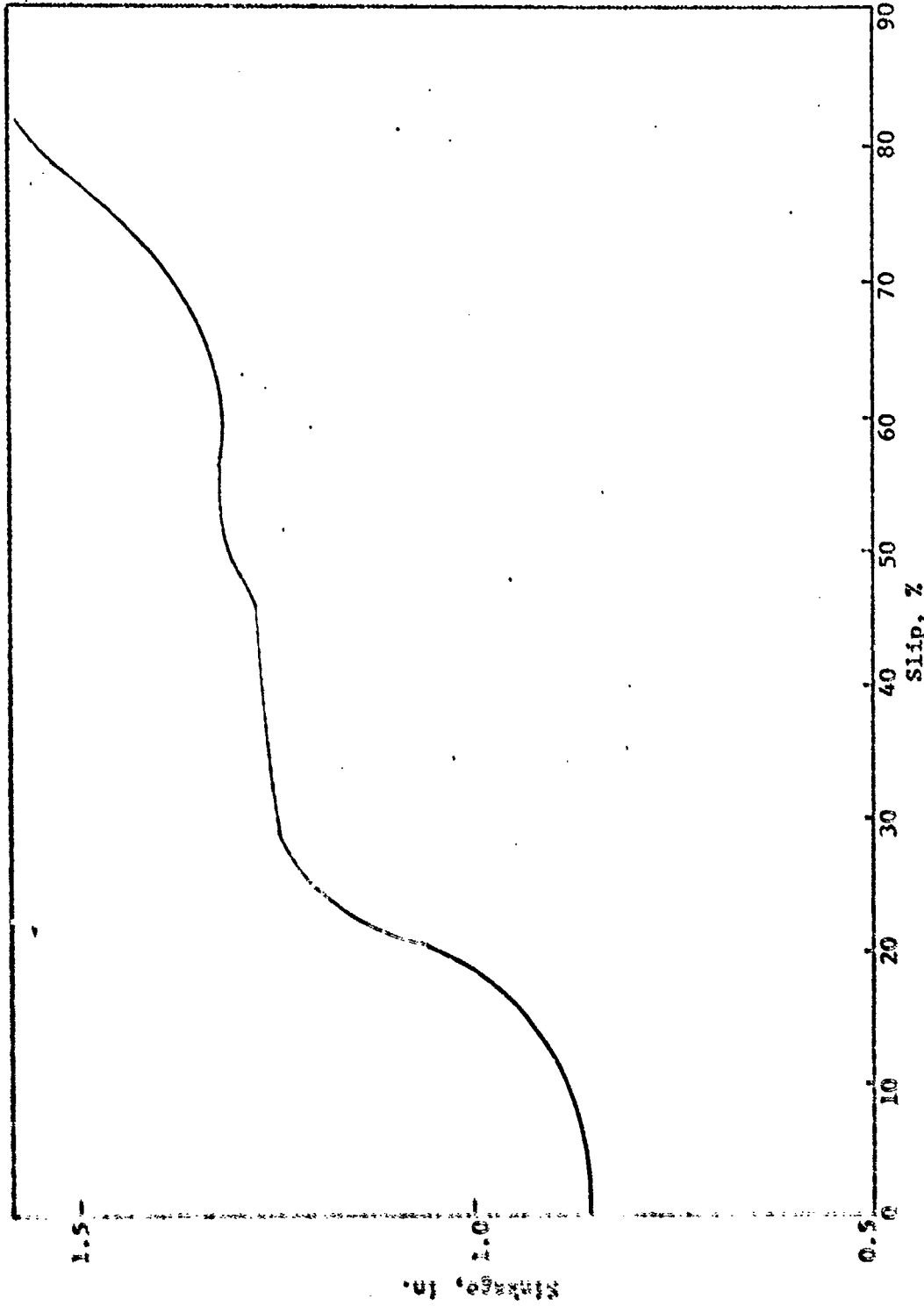


Fig. 15. Sinkage versus slip for the fabric-covered wheel (GM VII);
 wet sand $C_0 : C \approx 0.8$ psi/in.; $c = 0.04$ psi
 $w = 1.4\%$; load = 59 lb (260 N)

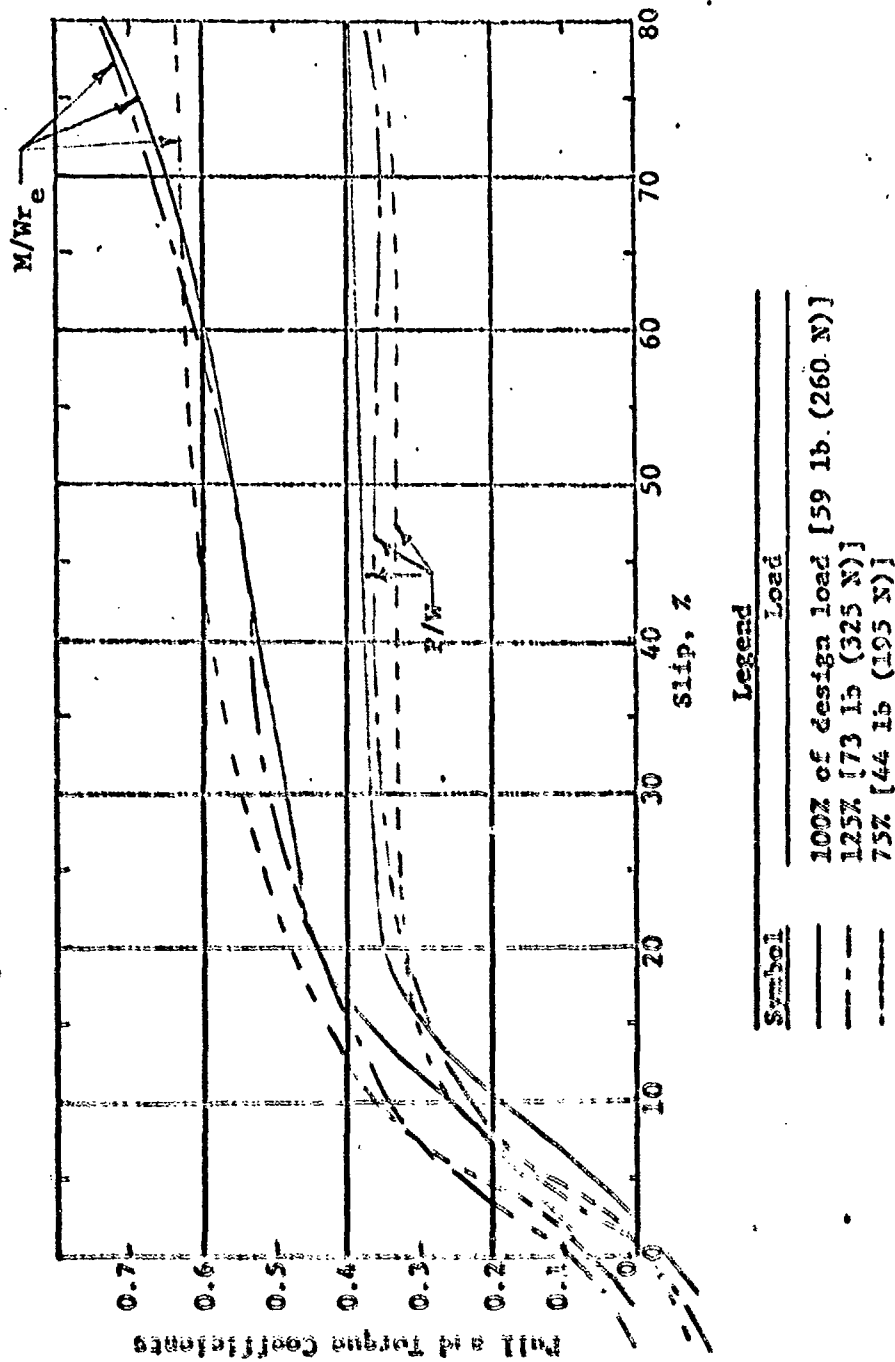


Fig. 16. Pull and torque coefficients versus slip for the open-mesh wheel (GM VIII);
 air-dry sand S_1 ; $C \approx 2.0$ psi/in.; $c = 0.0$ psi; $w < 0.5\%$

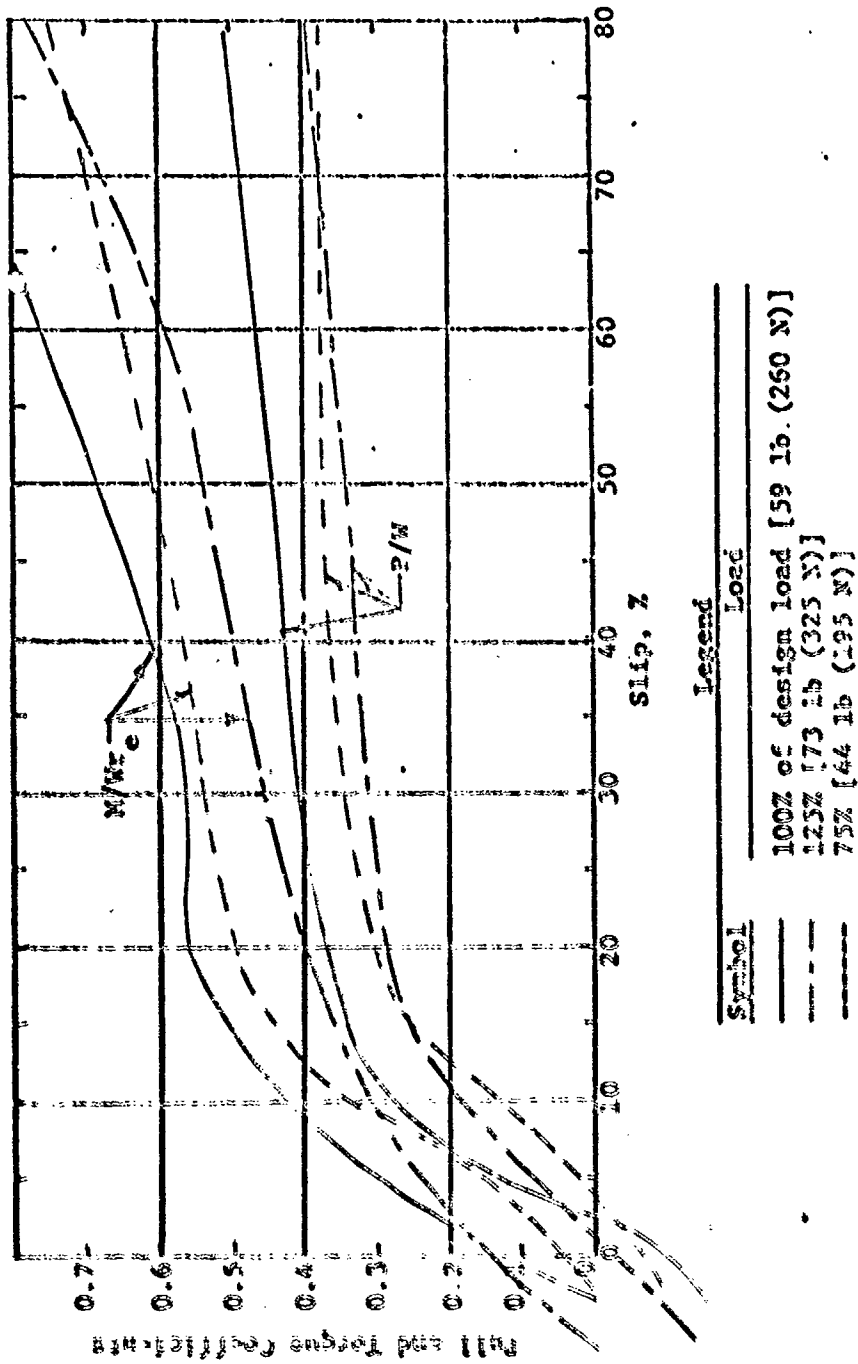


Fig. 17. Pull and torque coefficients versus slip for the open-mesh wheel (CM VIII); wet sand C_0 : $C = 0.8$ psi/in.; $c = 0.4$ psi; $w = 1.4\%$

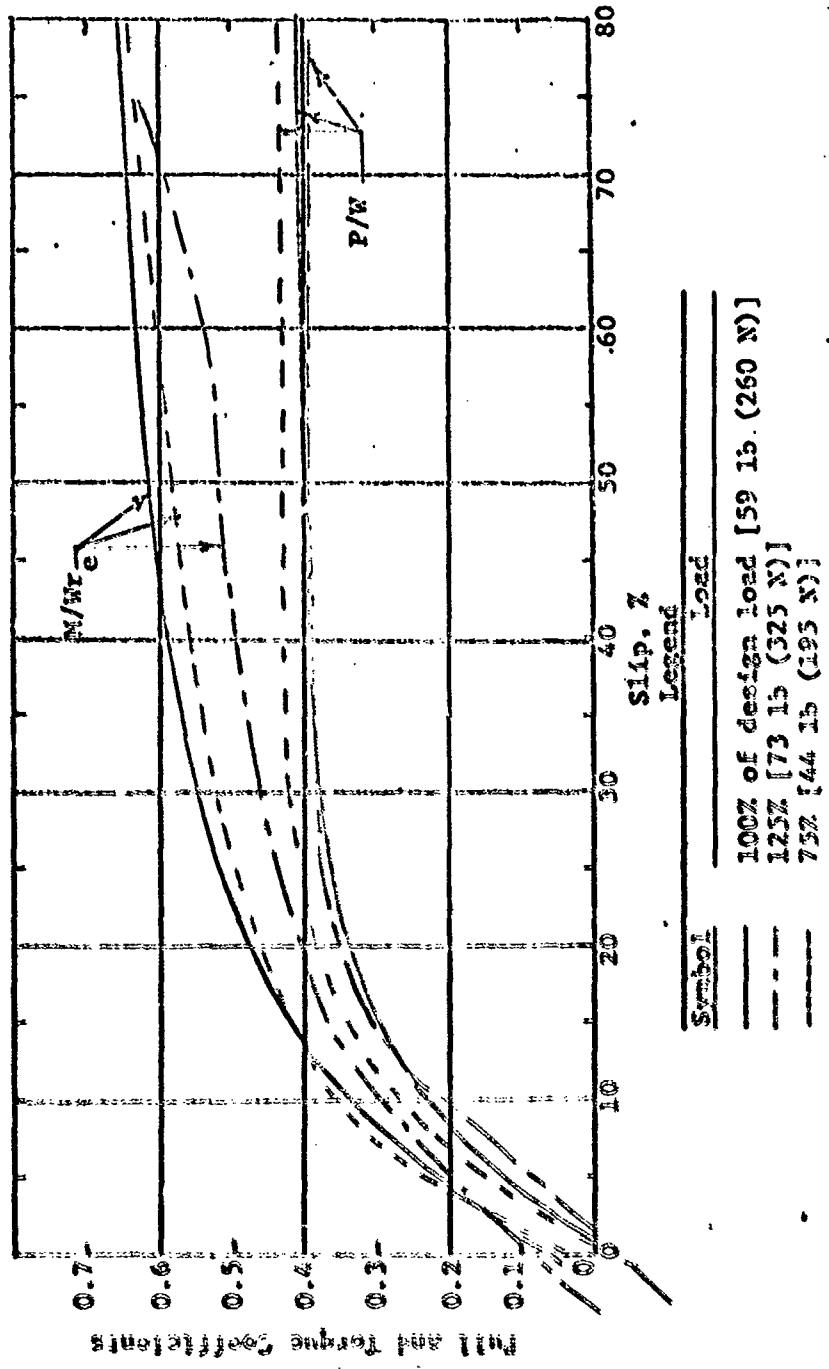


Fig. 18. Pull and torque coefficients versus slip for the open-mesh wheel (GM VIII); wet sand $C_1' : G = 4.9 \text{ psi/in.} ; c = 0.09 \text{ psi} ; w = 1.42$

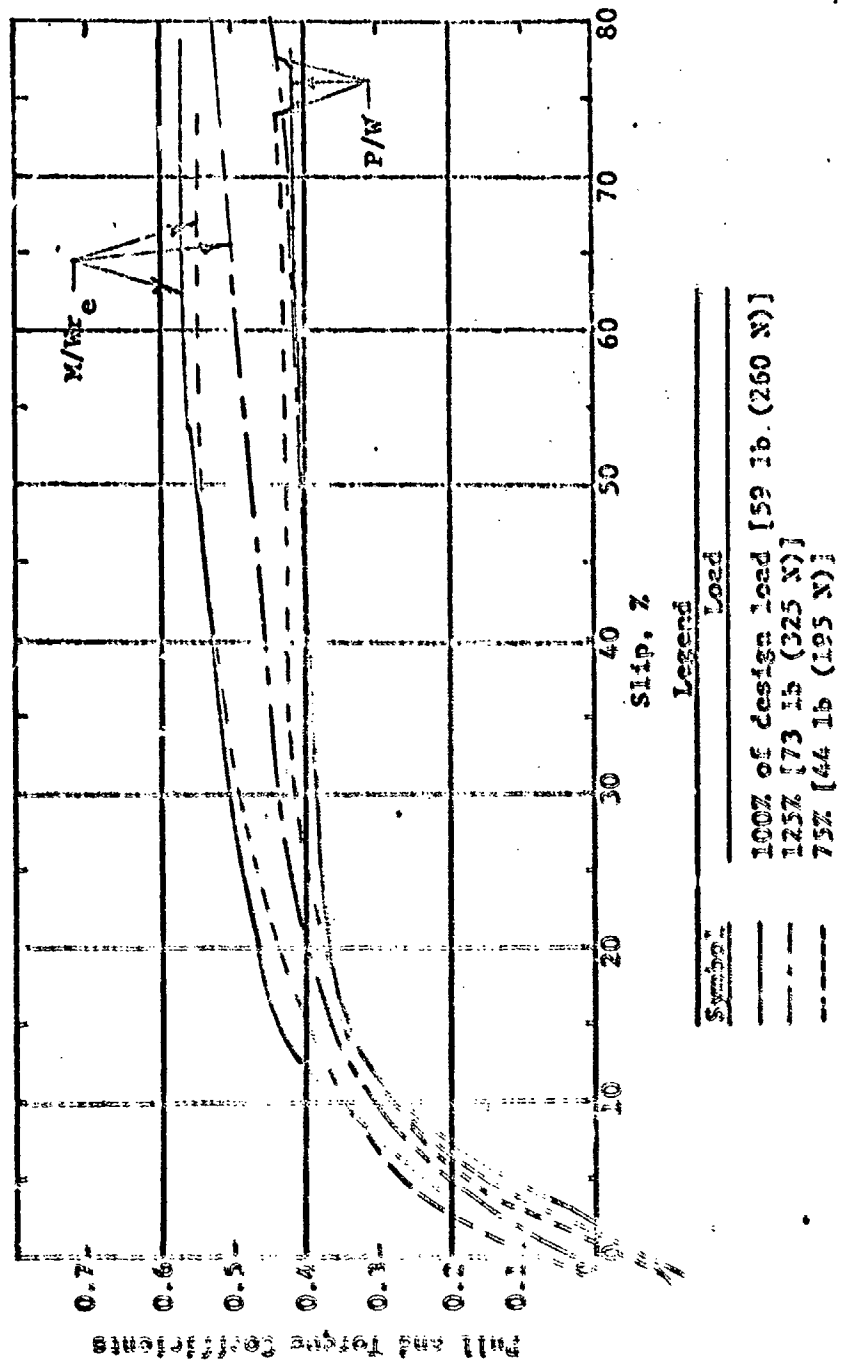
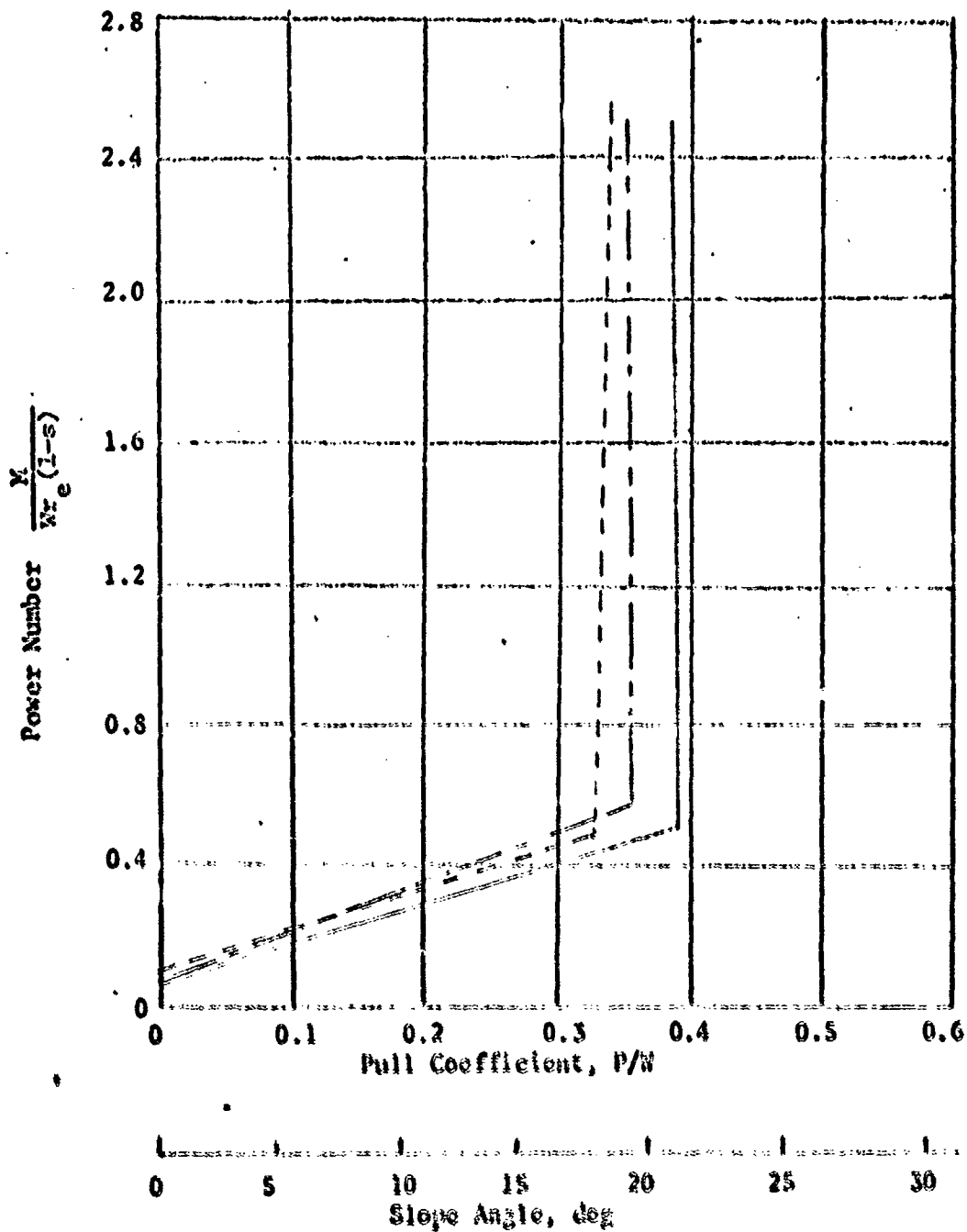
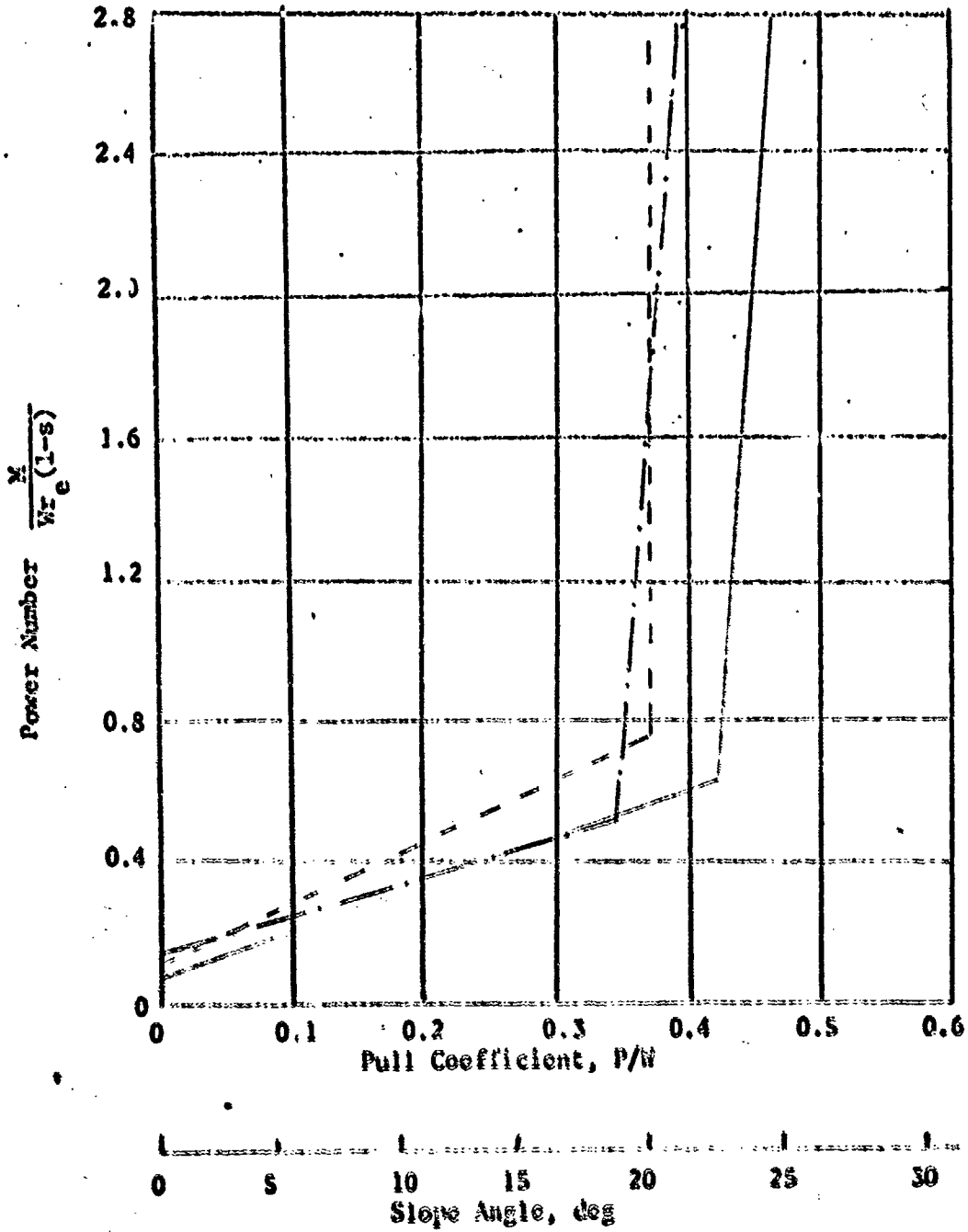


Fig. 19. Pull and torque coefficients versus slip for the open-mesh wheel (GM VIII); wet sand C_2 ; $G=2.0$ psi/in.; $c = 0.16$ psi; $w = 1.4\%$



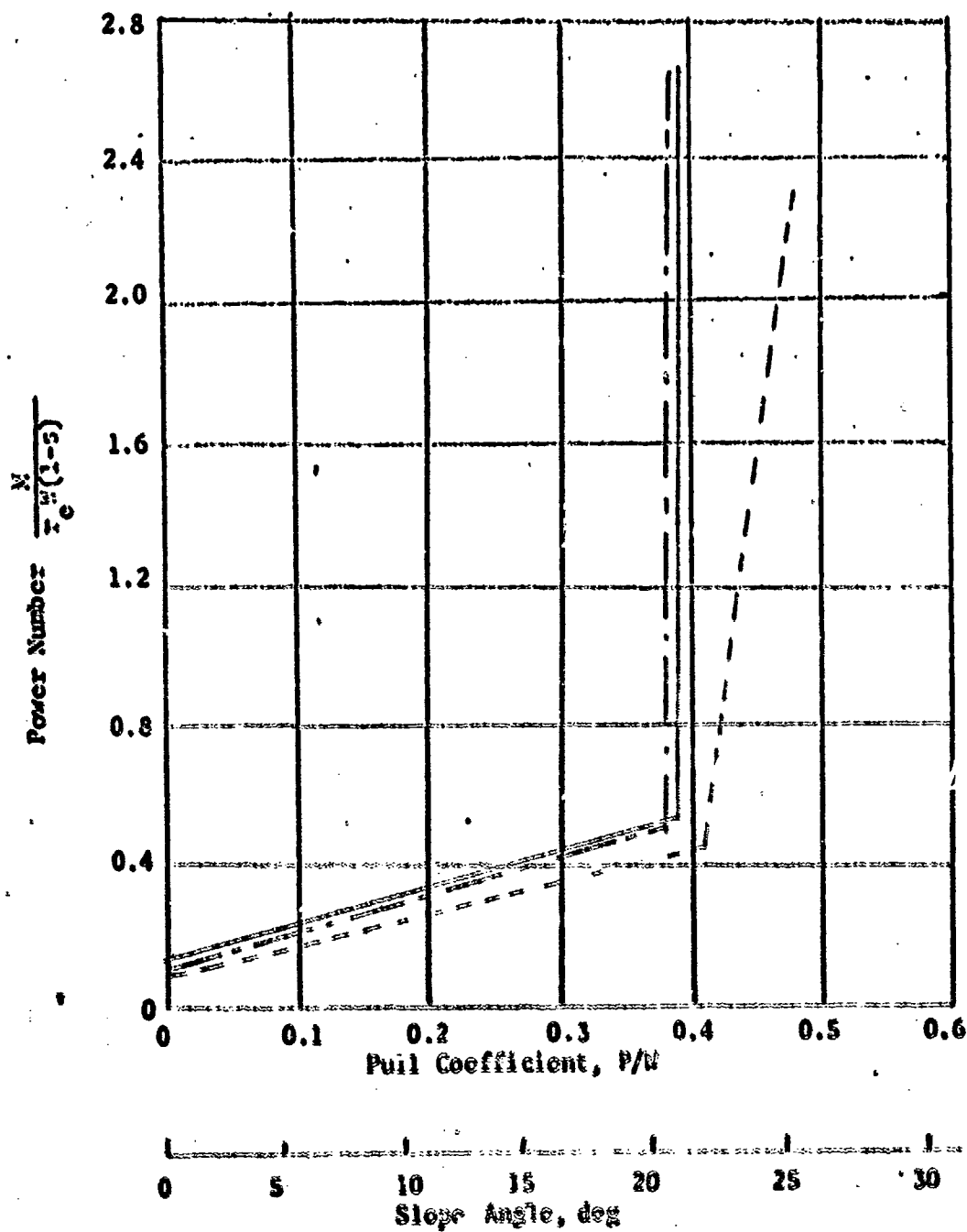
| Symbol | Load |
|-----------|-------------------------------------|
| — | 100% of design load (59 lb (260 N)) |
| - - - | 125% (73 lb (325 N)) |
| - · - · - | 75% (44 lb (195 N)) |

Fig. 20. Power number versus pull coefficient for the open mesh wheel (Cl VIII):
 air-dry sand $S_p : G \approx 2.0$ psi/in.; $c = 0.6$ psi; $v = 1.4\%$



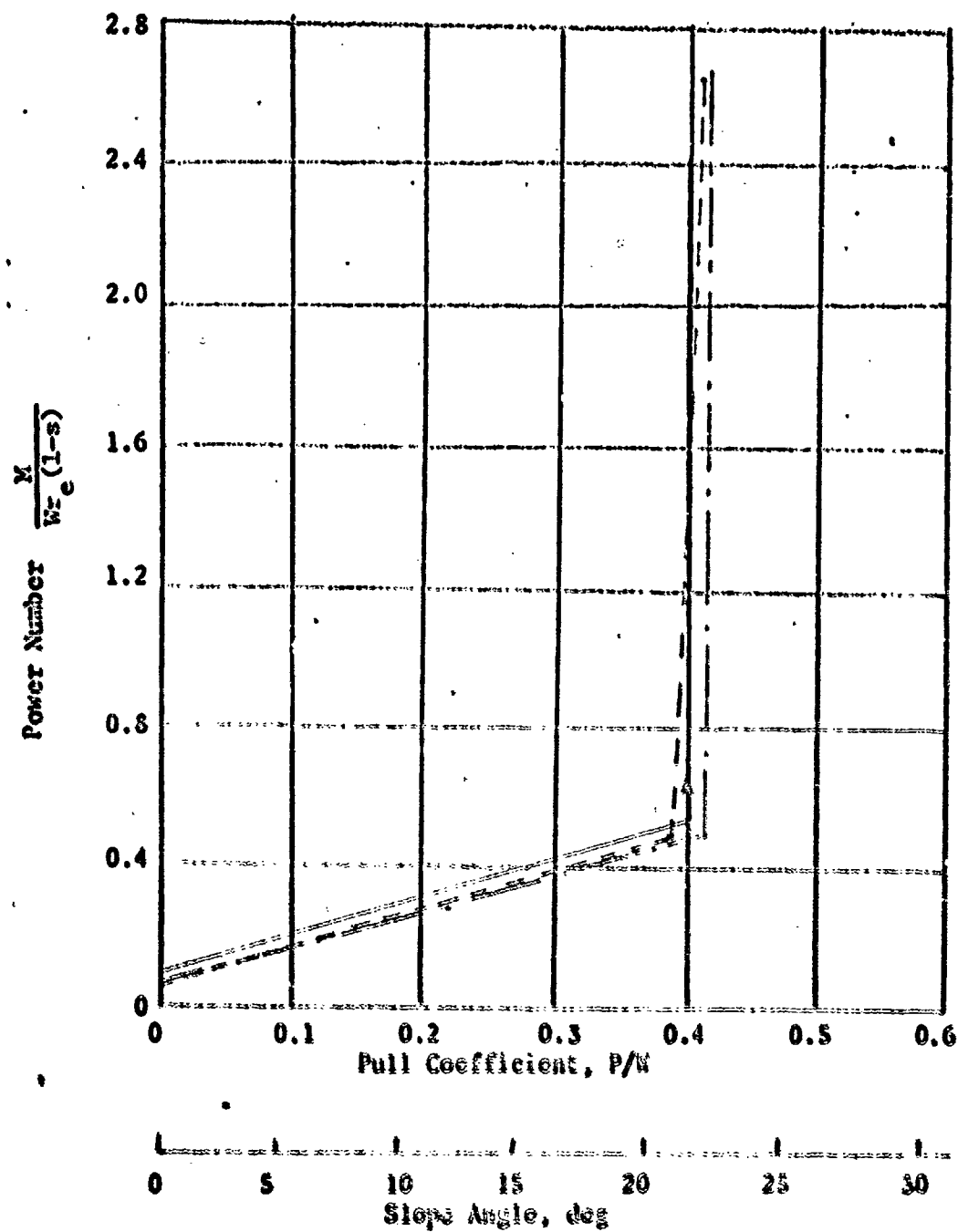
| Legend | |
|---------|-------------------------------------|
| Symbol | Load |
| — | 100% of design load [59 lb (260 N)] |
| - - - | 125% [73 lb (325 N)] |
| - · - · | 75% [44 lb (195 N)] |

Fig. 21. Power number versus pull coefficient for the open-back wheel (CX VIII): wet sand C_0 ; $C = 0.8$ psi/in.; $e = 0.04$ psi; $v = 1.6\%$



| Legend | |
|---------|-------------------------------------|
| Symbol | Load |
| — | 100% of design load [59 lb (260 N)] |
| - - - | 125% [73 lb (325 N)] |
| - · - · | 75% [44 lb (195 N)] |

Fig. 22. Power number versus pull coefficient for the open-mesh wheel (CI VIII); wet sand C_f ; $G = 4.9$ psi/ia.; $c = 0.09$ psi; $w = 1.4\%$



| Symbol | Load |
|-----------|-------------------------------------|
| — | 100% of design load [59 lb (260 N)] |
| - - - | 125% [73 lb (325 N)] |
| - · - · - | 75% [44 lb (195 N)] |

Fig. 23. Power number versus pull coefficient for the open-back wheel (C* VIII); wet sand $C_2 : C = 12.0$ psi/in.; $c = 0.16$ psi; $v = 1.4\%$



Fig. 24. Sand (≈ 25 lb (110 N)) trapped in open mesh wheel (accumulation of sand begins at approximately 10% slip)

1505-248

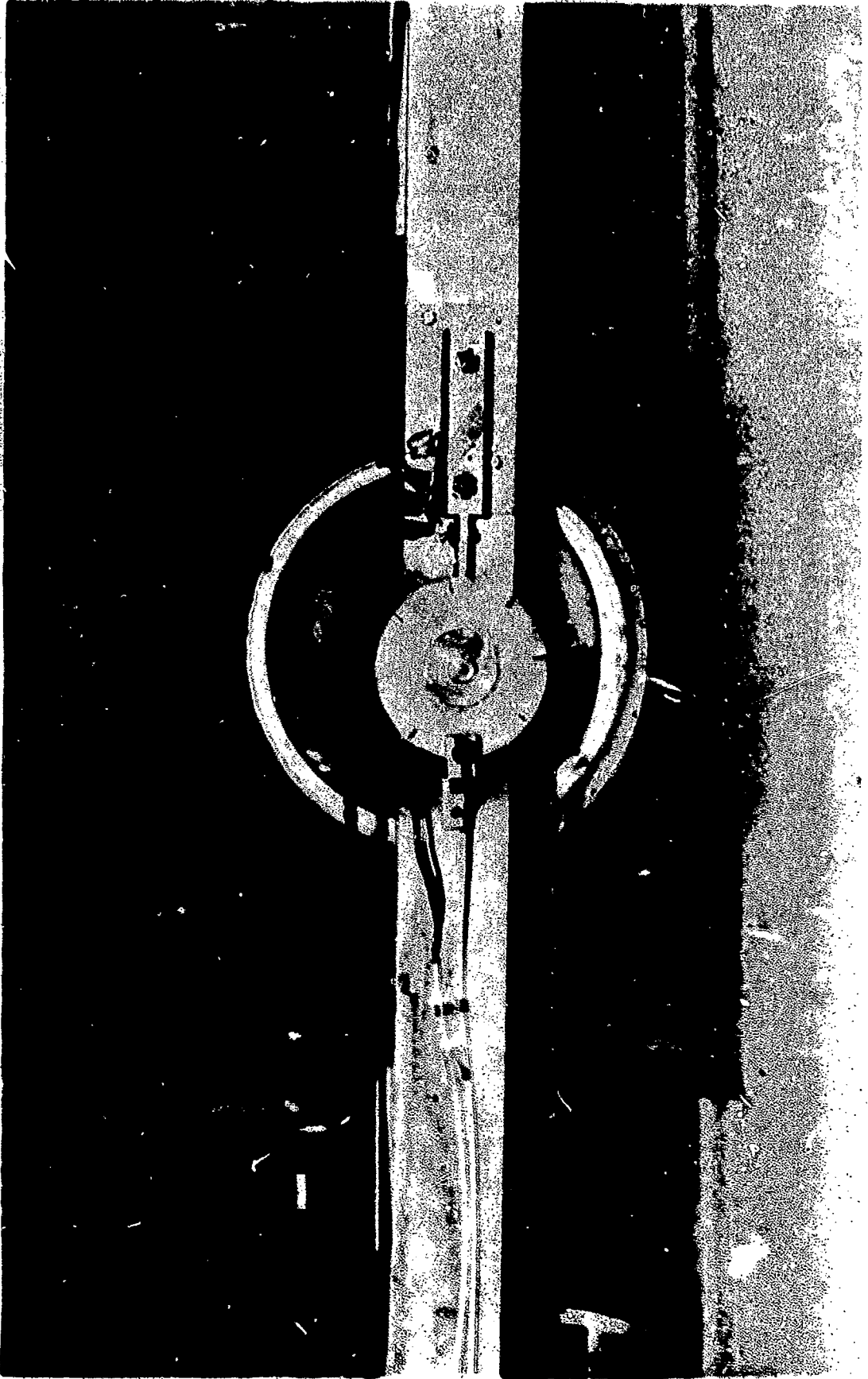


Fig. 25. Sand falling from open-mesh wheel at 210% slip

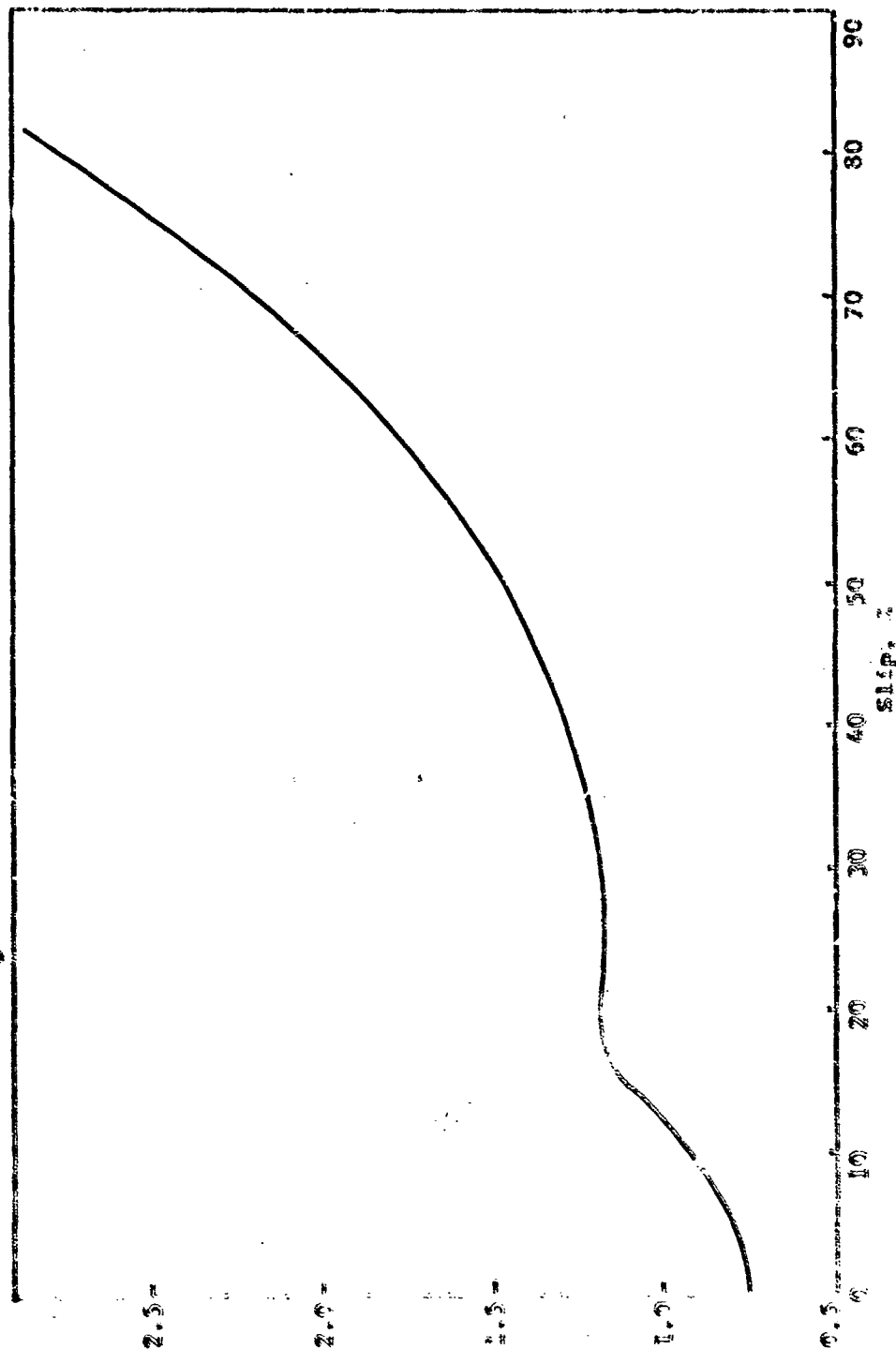


Fig. 26. Sinkage versus slip for the open-mesh wheel (GX VIII):
 Wet sand C_0 ; $C = 0.8$ psi/in.; $c = 0.4$ psi;
 $w = 1.4\%$; load = 59 lb (260 N)

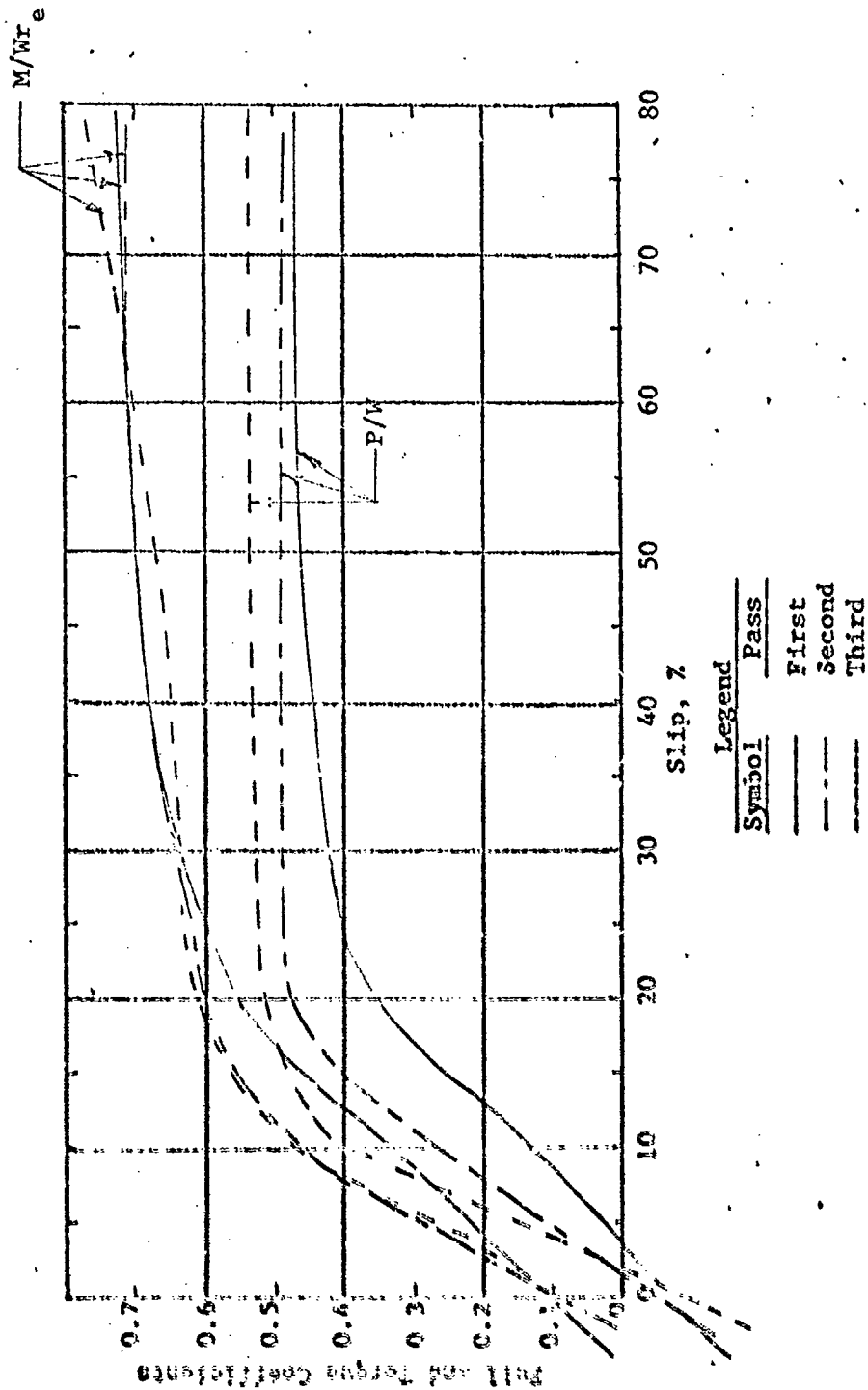


Fig. 27. Pull and torque coefficients versus slip for the fabric-covered (GM VII); wet sand $C_0 : C = 0.8$ psi/in.; $c = 0.04$ psi; $w = 1.4\%$; load = 59 lb. (260 N)

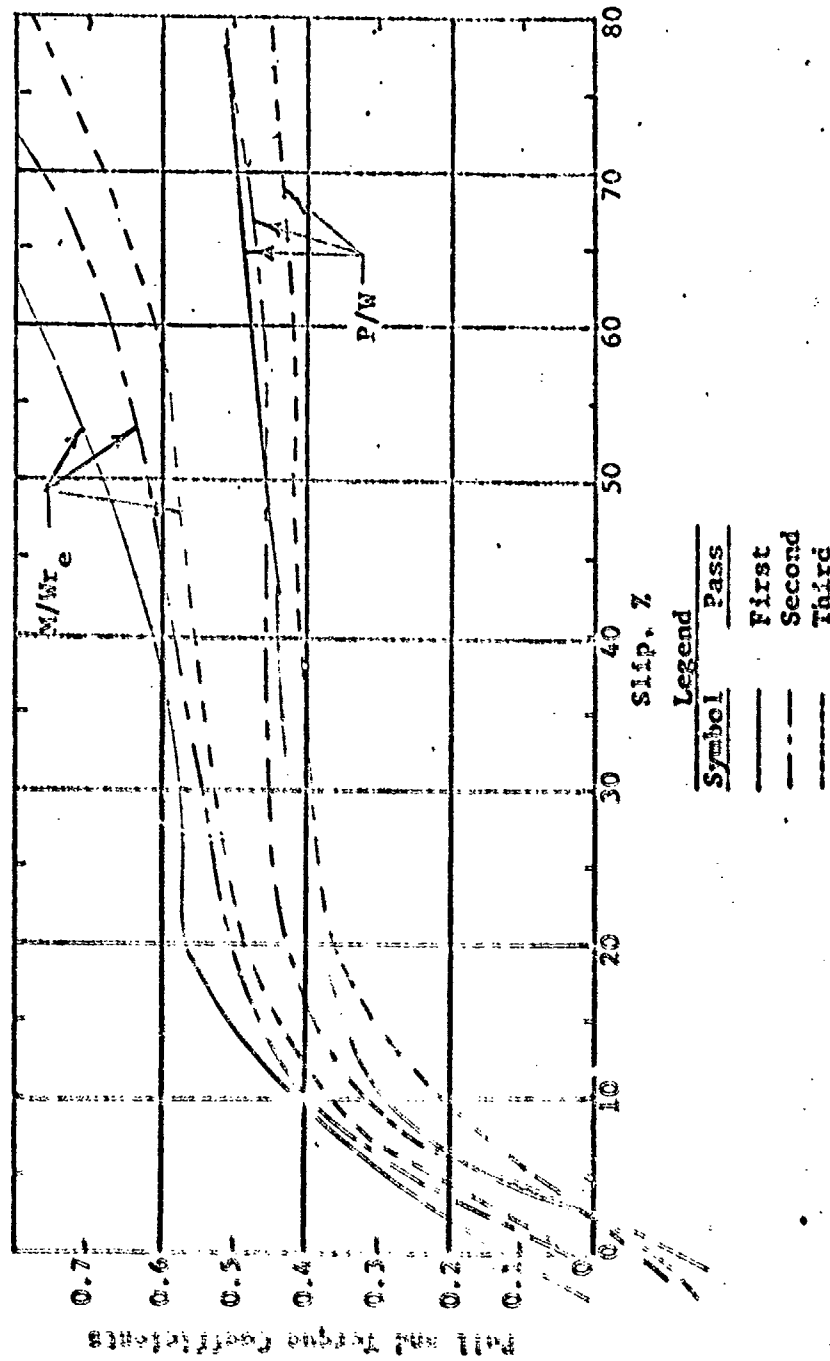


Fig. 28. Pull and torque coefficients versus slip for the open-mesh wheel (GM VIII) wet sand C_0 : $G = 0.8$ psi/in.; $c = 0.04$ psi; $w = 1.4\%$ load = 59 lb (260 N)